



Norwegian University of
Science and Technology

Simulation of Anchor Loads on Pipelines

Torunn Omnes Pettersen

Marine Technology

Submission date: June 2017

Supervisor: Svein Sævik, IMT

Co-supervisor: Erik Levold, Statoil

Norwegian University of Science and Technology
Department of Marine Technology



Norwegian University of
Science and Technology

Simulation of anchor loads on pipelines

Torunn Omnes Pettersen

Marine Technology

Submission date: 11.06.2017

Supervisor: Svein Sævik, IMT

Norwegian University of Science and Technology
Department of Marine Technology

PROJECT WORK FALL 2016

for

Stud. tech. Torunn Omnes Pettersen

Simulation of anchor loads on pipelines

Simulering av ankerlaster på rørledninger

Anchor loads on pipelines is in general a rarely occurring event, however, the severity when it occurs could easily jeopardize the integrity of any pipeline. It is considered as an accidental load in the design of pipelines. In the Norwegian Sea there are several locations where the subsea pipeline density is high, also in combination with high vessel density. The vessels usually know where pipelines are located and avoid anchoring, but anchors might be dropped in emergencies, lost in bad weather or due to technical failures. In these cases, the drop might not be noticed before the anchor hooks, e.g. in a pipeline.

Currently there is an ongoing project between DNV GL and Statoil to come out with a new recommended practice for anchor loads on pipelines. There have also been two master theses on the subject by Ying Wei (2015) and Kristbjörg Jónsdóttir (2016) focusing on numerical simulation of the anchor hooking event in SIMLA providing important input to the work. This is to be continued in this project and the work is therefore to be performed in close cooperation with Statoil with Dr. Erik Levold acting as a co-advisor.

One of the observations from the simulation carried out so far is that numerical problems might occur for the contact element CONT164 used so far. One of the goals of this project is to model the anchor geometry and contact by means of the new contact element CONT153 which was developed as part of Vegard Longvas PhD work.

The thesis work is to be carried out as a continuation of the project work carried out in 2016 and includes the following steps:

1. Literature study on pipeline technology, relevant standards for pipeline design, with particular focus on impact loads. Aspects related to vessel size, frequencies and corresponding anchor equipment is to be included also using previous thesis by Wei Ying and Stian Vervik as starting points.
2. Study the theoretical background for non-linear time domain contact modelling with focus on the formulations used in SIMLA, also get familiarized with the computer program SIMLA.
3. Define the basis for a case study considering anchor geometry, pipeline mechanical properties, soil interaction parameters, wire chain capacity, water depth, friction and hydrodynamic coefficients. This is to be done in closed cooperation with Statoil.
4. Establish SIMLA models for the hooking event using the CONT153 element that allows for sliding under friction along the pipeline and perform simulations to demonstrate the performance of the model as compared to the Jónsdóttir model .
5. Perform parametric studies with focus on 3D behaviour. Points that may be interesting to study when it comes to hooking / not hooking:

- Effects of the span height with respect to the hooking / non hooking
 - Anchor size, both in absolute terms and relative to the pipe it is towed over
 - Damping of the system in terms of whether or not the anchors are passing over the free span too easily
 - The effect of sloping seabed
 - The effect of friction between the anchor (steel) and tubes (typically concrete or sometimes the insulation coating)
 - The effect of towing speed 2 and 10 knots
 - Water depth 100 and 200 m
 - Seabed conditions (friction, burial)
 - Directionality 30 60 90
6. Points that may be interesting to study in terms of pipe global behavior (incl. Reversed bending):
- Anchor size, both in absolute terms and relative to pipe it towed over
 - The effect of towing speed
 - Water depth
 - Hydro dynamics (coefficients etc.)
 - Towing speed

Typical variation range for some parameters:

Pipe diameter: 16 inch to 42 inch, D / t : 25-45

Span Height: 0-2 m

Water depth: 100-250 m

Seabed conditions: axial friction factor: 0.2 to 0.8, lateral friction factor: 0.4 to 1.2

The above to be compiled into a set of parametric studies in agreement with the supervisors.

7. Conclusions and recommendations for further work

All necessary input data are assumed to be a combination of the ones used by Jónsdóttir and according to inputs from Statoil.

The work scope may prove to be larger than initially anticipated. Subject to approval from the supervisors, topics may be deleted from the list above or reduced in extent.

In the thesis the candidate shall present his personal contribution to the resolution of problems within the scope of the thesis work

Theories and conclusions should be based on mathematical derivations and/or logic reasoning identifying the various steps in the deduction.

The candidate should utilise the existing possibilities for obtaining relevant literature.

Thesis format:

The thesis should be organised in a rational manner to give a clear exposition of results, assessments, and conclusions. The text should be brief and to the point, with a clear language. Telegraphic language should be avoided.

The thesis shall contain the following elements: A text defining the scope, preface, list of contents, summary, main body of thesis, conclusions with recommendations for further work, list of symbols and acronyms, references and (optional) appendices. All figures, tables and equations shall be numerated.

The supervisors may require that the candidate, in an early stage of the work, presents a written plan for the completion of the work.

The original contribution of the candidate and material taken from other sources shall be clearly defined. Work from other sources shall be properly referenced using an acknowledged referencing system.

The report shall be submitted in two copies:

- Signed by the candidate
- The text defining the scope included
- In bound volume(s)
- Drawings and/or computer prints which cannot be bound should be organised in a separate folder.

Ownership:

NTNU has according to the present rules the ownership of the thesis. Any use of the thesis has to be approved by NTNU (or external partner when this applies). The department has the right to use the thesis as if the work was carried out by a NTNU employee, if nothing else has been agreed in advance.

Thesis supervisors:

Prof. Svein Sævik, NTNU

Dr. Erik Levold, Statoil

Deadline: December 16, 2016

Trondheim, August, 2016

Svein Sævik

Candidate – date and signature:

Preface

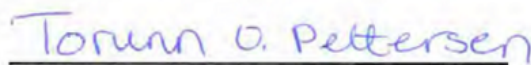
This report presents the results of my master thesis at the Norwegian University of Science and Technology. This thesis is a continuation of the research carried out during the spring semester of 2017. Both the project thesis and master thesis are mandatory parts of the Master program at the Institute of Marine Technology. The project work accounts for 7.5 credits and the master thesis accounts for 30 credits.

Currently, there is an ongoing project between DNV GL and Statoil to come out with a new recommended practice for anchor loads on pipelines. One of the observations from the simulation carried out so far is that numerical problems might occur for the contact element CONT164. One of the goals of this project is to model the anchor geometry and contact by means of the new contact element which was developed as part of Vegard Longva's PhD work at NTNU. The main topic of this thesis is to inspect how different parameters, like anchor size and water depth, affect the anchor-pipeline interaction. The simulations of the anchor-pipeline interaction were conducted using the computer software SIMLA. SIMLA was run in batch mode from MATLAB.

This project is a continuation of the master theses written by Stian Vervik (2011), Ying Wei (2015) and Kristbjörg Jónsdóttir (2016). MATLAB files were received from Jónsdóttir (2016).

I would like to thank my supervisor Prof. Svein Sævik at the Department of Marine Technology, NTNU, for guidance, feedback and involvement in the work. His knowledge about the computer program SIMLA has been of particularly help. I would also like to thank Dr. Erik Levold from Statoil for the input parameters and guidance, and I would like to acknowledge MARINTEK regarding the license of SIMLA. Finally, I would like to thank Kristbjörg Jónsdóttir for answering questions related to the MATLAB files.

Trondheim, June 2017



Torunn Omnes Pettersen

Abstract

Anchor loads on pipelines are in general a rarely occurring event, but the severity when it happens could easily jeopardize the integrity of any pipeline. The environmental and economic consequences of an accident caused by dragging anchors could be substantial. The offshore pipeline density at several locations in the North Sea is high. High pipeline density combined with high vessel density increase the risk of accidents related to anchor-pipeline interaction.

Currently, there is an ongoing project between DNV GL and Statoil to come out with a new recommended practice for anchor loads on pipelines. The research on anchor-pipeline interaction is quite limited, however some studies on dropped and dragged anchors are conducted. The studies on the subject anchor-pipeline interactions primarily focus on the potential damage an anchor may inflict on a pipeline, the replacement length when accidents happen and risk studies.

One of the observations from the simulations of anchor-pipeline interactions carried out so far is that numerical problems might occur for the contact element CONT164. One of the goals of this work was to establish models for the hooking event using a new contact element developed by Vegard Longva as part of his PhD work at NTNU. Simulations of eleven models were conducted to demonstrate the performance of the new contact element. 55 % of the models showed unrealistic behavior when the anchor-pipeline interaction was modelled with the old contact element, CONT164. A simulation was classified as unrealistic if the anchor pierced the pipeline, or if the anchor grossly deformed. All models tested showed a realistic behavior when the anchor geometry and contact were modelled with the new contact element.

The objective of this thesis is to study the behavior of the anchor when it collides with an offshore pipeline. A parametric study was performed to investigate the response of the anchor. 250 simulations of anchor-pipeline interactions were performed. The parameters investigated were vessel velocity, pipe diameter, anchor size, span height, damping of the system, sloping seabed, seabed conditions, angle of attack between the anchor and the pipeline and water depth. The pipeline was modelled as a ten-meter-long constrained rigid body in the parametric study. The parametric study indicated that the probability of an anchor hooking onto a pipeline increases with decreasing vessel speed, decreasing pipe diameter and increasing anchor size. The trend is that the hooking ratio increases with increasing anchor mass. However, it is not given that a large anchor hooks onto a pipeline even though a smaller anchor did hook onto the same pipeline. The hooking ratio is highest when the pipeline is partly buried. Increasing the span height decreases the hooking ratio. None of the models hooked the pipeline in the parametric study when the angle of attack between the anchor and the pipeline was 30 or 60 degrees.

24 case studies were performed to investigate how well the anchor's response had been predicted in the parametric study. The pipeline was modelled as ten-kilometers-long and the pipeline was only constrained at the end nodes. In general, the parametric study was good at predicting the response of the anchor-pipeline interaction when the pipeline was not in free span.

Sammendrag

Ulykker der undersjøiske rørledninger utsettes for ankerlaster forekommer sjeldent, men alvorlighetsgraden er høy når ulykker av denne typen inntreffer. De miljømessige og økonomiske konsekvensene av en ulykke forårsaket av et anker som hekter seg i en rørledning kan være betydelige. Tettheten av undersjøiske rørledninger er høy i Nordsjøen. Høy tetthet av undersjøiske rørledninger kombinert med mye skipstrafikk øker risikoen for ulykker der rørledninger blir utsatt for ankerlaster.

DNV GL og Statoil arbeider med en ny standard for ankerlaster på rørledninger. Antall studier på kollisjoner mellom anker og undersjøiske rørledninger er begrenset. Studiene som er gjennomført fokuserer i hovedsak på skadene et anker kan påføre en rørledning, hvor stor del av rørledningen som må byttes ut hvis den blir utsatt for ankerlaster og risiko for at ulykker skjer.

Simuleringer av interaksjon mellom anker og rørledninger i SIMLA har vist at numeriske problemer kan oppstå når kontaktelementet CONT164 blir benyttet. Et av målene med dette arbeidet er å lage en ny modell av interaksjonen mellom anker og rørledning der et nytt kontaktelement, utviklet av Vegard Longva som del av hans doktorgrad ved NTNU, blir benyttet. Elleve simuleringer av interaksjon mellom anker og rørledning ble gjennomført for å demonstrere bruken av det nye kontaktelementet. 55 % av modellene viste en urealistisk respons når kontakten mellom ankeret og rørledningen ble modellert med det gamle kontaktelementet, CONT164. En simulering ble kategorisert som urealistisk hvis ankeret gjennomboret rørledninger, eller hvis ankeret ble svært deformert. Alle simuleringene ble kategorisert som realistiske når kontakten mellom ankeret og rørledningen ble modellert med det nye kontaktelementet.

Hovedmålet med denne masteroppgaven var å studere ankerets oppførsel når det kolliderte med en undersjøisk rørledning. En parameterstudie ble gjennomført for å undersøke ankerets oppførsel. 250 simuleringer av interaksjon mellom anker og rørledning ble gjennomført. Parametrene som ble undersøkt var ankermasse og -geometri, diameter på rørledning, ankerets angrepsvinkel, tauehastighet, spennhøyde, vann dybde og havbunnsforhold. Den undersjøiske rørledningen ble modellert som et 10 meter langt fast innspent stivt legeme i parameterstudien. Resultatene fra parameterstudiet viser en økning i «hooking»-responser ved økt ankermasse, lavere tauehastighet og mindre rørdiameter. Trenden er at «hooking»-forholdet øker med økende ankermasse. Det er imidlertid ikke gitt at et stort anker fester seg i en undersjøisk rørledning selv om et mindre anker festet seg i den samme rørledningen. Det største antall «hooking»-responser er observert når rørledningen er delvis nedgravd i sjøbunnen. Å øke rørledningens spennhøyde minker sjansen for at ankeret fester seg i rørledningen. Ingen interaksjoner resulterte i en «hooking»-respons i parameterstudien når angrepsvinkelen mellom ankeret og rørledningen var 30 eller 60 grader.

24 casestudier ble utført for å undersøke hvor godt ankerets respons ble anslått i parameterstudien. Rørledningen ble modellert 10 kilometer lang med elastoplastiske materialegenskaper. Røret var kun fast innspent ved endene. Simuleringene viste at ankerets respons ble godt anslått i parameterstudien så lenge ankeret ikke var i fritt spenn.

Contents

Preface	II
Abstract	IV
List of Figures	X
List of Tables	XII
Nomenclature	XIV
1 Introduction	1
1.1 Motivation	1
1.2 Objective	1
1.3 Scope and limitations	1
1.4 Chapter overview	2
2 DNV GL rules and regulations	3
2.1 DNV-OS-F101: Submarine pipeline systems	3
2.2 DNV-RP-F111: Interference between trawl gear and pipelines	6
2.3 DNV-RP-F107: Risk assessment of pipeline protection	6
2.4 DNVGL-OS-E301: Position mooring	8
3 Literature review	9
3.1 Research papers	9
3.2 Geometrical consideration of the anchor hooking problem	11
3.3 Master theses	13
3.3.1 Pipeline accidental load analysis	13
3.3.2 Anchor loads on pipelines	14
3.3.3 Simulation of anchor loads on pipelines	15
4 Non-linear finite element analysis	18
4.1 Basic principles of structural analysis	18
4.1.1 Equilibrium	18
4.1.2 Kinematic compatibility	18
4.1.3 Material law	19
4.2 Non-linear effects	21
4.3 Solution methods	21
4.3.1 Static solution	21
4.3.2 Dynamic solution	22
4.4 Finite element formulation	22
5 Modelling	23
5.1 Pipe elements	23
5.1.1 Pipeline	24
5.1.2 Chain	25
5.2 Anchor	26
5.3 Soil	26
5.3.1 Material curve in y-direction	26

5.3.2	Material curve in z-direction	27
5.4	Contact elements	27
5.4.1	Interaction between physical objects and the sea floor	28
5.4.2	Contact between anchor chain and pipeline	28
5.4.3	Contact between anchor and pipeline	29
6	Specifics of analyses	31
6.1	Comparison study	31
6.2	Parametric study	31
6.3	Case studies	33
7	Results and discussion	34
7.1	Comparison study	34
7.2	Parametric study	37
7.2.1	The pipeline is resting on a flat seabed	37
7.2.2	The span height of the pipeline is two meters and the seabed is flat	39
7.2.3	The pipeline is partly buried in the seabed	43
7.2.4	The effect of sloping seabed	46
7.2.5	30 and 60 degrees angle of attack between the anchor and the pipeline	47
7.2.6	Summary of the parametric study	48
7.2.7	Pipeline forces	51
7.3	Elastoplastic case studies	53
8	Conclusion	57
9	Further work	58
	Bibliography	59
A	Results from parametric study: Pipeline is resting on a flat seabed	I
B	Results from parametric study: The span height of the pipeline is two meters and the seabed is flat	IV
C	Results from parametric study: The pipeline is partly buried in the seabed	VII
D	Results from parametric study: Sloping seabed	X
E	Results from the parametric study: 30 and 60 degrees angle of attack between the anchor and the pipeline	XIII
F	Calculations for pipe elements	XVI
G	Electronic appendix	XIX

List of Figures

- 1 Process description of risk assessment (DNV-RP-F107, 2010) 7
- 2 Spek anchor (SOTRA, 2014a) 11
- 3 Hooked pipe section (Nord Stream, 2008) 12
- 4 The distribution of anchor classes for the vessels able to hook the Kvitbjørn pipeline. 14
- 5 Stress-strain relationship. σ_y is the stress at the first onset of yielding (Moan, 2003) 20
- 6 Model of the anchor-pipeline interaction (Jónsdóttir, 2016) 23
- 7 Degrees of freedom for a pipe element (Sævik, 2008) 23
- 8 Stud Link Chain (SOTRA, 2014b) 25
- 9 Anchor models 26
- 10 Geometrical relations for roller contact element. Figure: (Sævik, 2008) 28
- 11 Current configuration of pipe and body (Longva and Sævik, 2013). 29
- 12 Definition of angle of attack between the pipeline and the anchor. 31
- 13 Naming system (Jónsdóttir, 2016) 34
- 14 Categorization of the anchor-pipeline interaction. 34
- 15 Example of a pull over response 35
- 16 Example of a bounce over response 35
- 17 The bar plot shows how the hooking ratio depends on anchor size and water depth when the pipeline is resting on a flat seabed 37
- 18 The anchor-pipeline interaction for model 6000kg200m30in10kn578m90 (A) 38
- 19 The anchor-pipeline interaction for model 7800kg200m30in10kn633m90 (B) 38
- 20 The bar plot shows how the hooking ratio depends on pipe diameter and vessel velocity when the pipeline is resting on a flat seabed. 39
- 21 The bar plot shows how the hooking ratio depends on anchor size and water depth when the span height of the pipeline is two meters. 39
- 22 The anchor-pipeline interaction for model 6000kg200m30in2kn578m90 40
- 23 The anchor-pipeline interaction for model 7800kg200m30in2kn633m90 40
- 24 The bar plot shows how the hooking ratio depends on pipe diameter and vessel velocity when the span height of the pipeline is two meters. 41
- 25 The anchor-pipeline interaction for model 15400kg200m30in10kn743m90 42
- 26 Element force in anchor chain element 50002 for model 15400kg200m30in10kn743m90. The element force is given in megapascal and the time is given in seconds. 42
- 27 The bar plot shows how the hooking ratio depends on anchor size and water depth when the pipeline is partly buried. 43
- 28 The anchor-pipeline interaction for model 4890kg100m30in2kn550m90 44
- 29 The anchor-pipeline interaction for model 4890kg100m30in2kn550m90. The pipeline is partly buried in the seabed. 44
- 30 The anchor-pipeline interaction for model 4890kg100m30in2kn550m90. The pipeline is resting on the seabed. 45
- 31 The bar plot shows how the hooking ratio depends on pipe diameter and vessel velocity when the pipeline is partly buried. 45
- 32 The bar plot shows how the hooking ratio depends on anchor size and water depth when the seabed is inclined at five degrees with respect to the horizontal. 46

33	The bar plot shows how the hooking ratio depends on pipe diameter and vessel velocity when the seabed is inclined at five degrees with respect to the horizontal.	47
34	The position of the anchor as it gets dragged over the pipeline. The angle of attack between the anchor and the pipeline is 30 degrees.	47
35	Hooking ratio when the angle of attack is 90 degrees. A: The pipeline is resting on a flat seabed, B: The span height of the pipeline is two meters and the seabed is flat, C: The pipeline is partly buried in a flat seabed, D: The seabed is inclined at five degrees with respect to the horizontal.	48
36	The bar plot shows how the hooking ratio depends on anchor size.	49
37	The bar plot shows how the hooking ratio depends on pipe diameter.	49
38	The bar plot shows how the hooking ratio depends on vessel velocity.	50
39	The bar plot shows how the hooking ratio depends on water depth.	51
40	The plot shows how the pipeline forces vary over time for the model 6000kg200m40in10kn578m90.	52
41	The plot shows how the pipeline forces vary over time for the model 6000kg100m40in2kn578m90.	52
42	The plot shows how the pipeline forces vary over time for the model 6000kg100m30in2kn578m90.	53
F.1	Simplified Anchor Geometry (Jónsdóttir, 2016)	XVI

List of Tables

- 3 Typical link between scenarios and limit states. 4
- 4 Equipment table, (DNVGL-OS-E301, 2015) 8
- 5 Lateral force limits for pipeline resting on a seabed (Sriskandarajah and Wilkins, 2002) 9
- 6 Lateral force limits for pipeline partially buried (Sriskandarajah and Wilkins, 2002) 9
- 7 Dimensions (figure 2) for different anchor masses (SOTRA, 2014a) 11
- 8 Maximum hooking diameter for Spek anchors 12
- 9 Equipment letter parameters. A variety of anchor sizes and the associated chain parameters. (Vervik, 2011) 13
- 10 Anchor classes (Vervik, 2011) 13
- 11 Parameters inspected by Wei (2015) 14
- 12 Parameters investigated by Jónsdóttir (2016) 15
- 13 Hooking ratio distribution (Jónsdóttir, 2016) 16
- 14 Overview of results in the parametric study (Jónsdóttir, 2016) 16
- 15 Minimum required anchor chain length (Jónsdóttir, 2016) 16
- 16 Important pipeline parameters 24
- 17 Boundary conditions for the pipeline 25
- 18 Parameters investigated 32
- 19 Span length 33
- 20 Results from simulations, comparison study 36
- 21 Results of the elastoplastic case study. The pipeline is resting on the sea floor. 53
- 22 Results of the elastoplastic case studies. The pipeline is partly buried in the seabed. 54
- 23 Results of the elastoplastic case studies. The span height is two meters. . . 54
- 24 The effect of damping. Model: 7800kg100m30in10kn633m90, The pipeline is resting on a flat seabed. 55
- 25 The effect of damping. Model: 9900kg200m30in10kn660m90, the pipeline is partly buried in a flat seabed. 55
- 26 The effect of damping. Model: 9900kg200m40in2kn633m90, the span height of the pipeline is two meters and the seabed is flat. 55
- 27 The effect of damping. Model: 15400kg200m40in10kn743m90, the span height of the pipeline is two meters and the seabed is flat. 55
- A.1 Results of th parameric study when the pipeline is resting on a flat seabed I
- B.1 Results from the parametric study when the span height of the pipeline is two meters and the seabed is flat IV
- C.1 The results from the parmetric study when the seabed is flat and the pipeline is partly buried in the seabed VII
- D.1 The results from the parametric study when the seabed is inclined at 5 degrees with respect to the horizontal X

E.1	The results of the parametric study when the angle of attack between the anchor and the pipeline is 30 degrees and 60 degrees. The seabed is flat and the pipeline is resting on the sea floor. The cases are labeled "Error" if the simulation stopped before it was possible to conclude whether the anchor would pull over, bounce over or hook the pipeline. The cases are labeled with a * if it is impossible to conclude whether the brief contact was a bounce over or pull over response.	XIII
F.1	Anchor calculations	XVI
F.2	Anchor chain calculations	XVII
F.3	Pipeline calculations	XVIII
G.1	Content of the electronic appendix, uploaded to DIVA	XIX

Nomenclature

Abbreviations

ALARP	as-low-as-reasonably-possible
ALS	Accidental Limit State
DNV	Det Norsk Veritas
FLS	Fatigue Limit State
LRFD	Load and Resistance Factor Design
MARINTEK	Norwegian Marine Technology Research Institute
NTNU	Norwegian Univeristy of Science and Technology
SLS	Serviceability Limit State
ULS	Ultimate Limit State

Symbols – latin characters

A	Projected area
C	Damping matrix
C_A	Added mass coefficient
C_D	Drag coefficient
D	Nominal outside diameter
D_{fat}	Miner's sum
DFE	Design fatigue factor
EN	Equipment number
g_0	Initial gap
H_p	Permanent plastic dent depth
k	Number of stress blocks
K	Stiffness matrix
L	Length of fluke
L_A	Load effect from accidental load
L_E	Load effect from environmental load
L_F	load effect from functional loads
L_I	Load effect from interference load
L_{Sd}	Design load effect
m_a	Added mass
M	Mass damping matrix
M_p	Plastic capacity
M_{Sd}	Design moment
n	Normal vector
n_i	Number of stress cycles in stress block i
N	Normal contact force
N_i	Number of cycles to failure at constant stress range
p_b	pressure containment resistance
p_c	characteristic collapse pressure
p_e	External pressure
p_h	Mill test pressure
p_{li}	Local incidental pressure
p_{min}	Minimum internal pressure

Q	Load vector
r	displacement vector
R	Load vector
Re	Reynolds number
S	Force matrix
S_{sd}	Design effective axial force
t	Time
u_x	Displacement in X-direction
u_y	Displacement in Y-direction
u_z	Displacement in Z-direction
u	Displacement field
v	Displacement vector
x	Coordinates

Symbols – greek characters

α	The angle between the fluke and the shank
α_1	Mass damping ratio
α_2	Stiffness damping ratio
α_c	Flow stress parameter
α_{mpt}	Mill pressure test factor
α_{spt}	System pressure test factor
α_u	Material strength factor
γ_A	Load effect factor for accidental load
γ_c	condition load effect factor
γ_E	Load effect factor for environmental load
γ_F	Load effect factor for functional load
γ_m	material resistance factor
γ_{SC}	Safety class resistance factor
Δ	Displacement
ϵ_{11}	Principal strain
ϵ_{22}	Principal strain
ϵ_c	Characteristic bending strain resistance
ϵ_{sd}	Design load strain
η	Poisson's ratio
κ	Strain-hardening parameter
θ_x	Rotation about X-axis
θ_y	Rotation about Y-axis
θ_z	Rotation about Z-axis
η	Usage factor
σ_{11}	Principal stress
σ_{22}	Principal stress
σ_y	Yield strength
ω_0	Natural frequency

1 Introduction

1.1 Motivation

Interaction between dragging anchors and offshore pipelines is one of the most serious accidents that pipelines experience. The environmental and economic consequences could be substantial. The offshore pipeline density at several locations in the North Sea is high. High pipeline density combined with high vessel density increase the risk of accidents related to anchor-pipeline interaction. The vessels usually know where the offshore pipelines are located and avoid anchoring in these locations, but anchors might be dropped in emergencies, lost in bad weather or due to technical failures. Dragging anchors may cause rupture of the pipeline due to large bending deformation combined with a large axial force. The production has to be stopped immediately when a pipeline ruptures to reduce the consequences, and required repair must be undertaken.

1.2 Objective

Currently, there is an ongoing project between DNV GL and Statoil to come out with a new recommended practice for anchor loads on pipelines. The research on anchor-pipeline interaction is quite limited, however some studies on dropped and dragged anchors are conducted. The studies on the subject anchor-pipeline interactions primarily focus on the potential damage anchor may inflict on a pipeline, the replacement length when accidents happen and risk studies. The main objective of this thesis is to determine how different parameters, like anchor size and towing velocity, affect the anchor's behavior when it collides with a subsea pipeline. The result of this thesis will provide input to the ongoing project between DNV GL and Statoil.

1.3 Scope and limitations

Three master theses have previously been written at the institute of Marine Technology at NTNU related to the subject anchor loads on pipelines. Vervik's master thesis (2011) is based on the anchor hooking incident at the Kvitebjørn Gas Pipeline. Wei (2015) and Jónsdóttir (2016) focused on numerical simulation of the anchor hooking event in the computer software SIMLA. This master thesis is a continuation of this work. The project is to be performed in cooperation with Statoil.

One of the goals of this project is to model the anchor geometry and contact by means of the new contact, CONT153, which was developed as part of Vegard Longva's PhD work at NTNU. Simulations of the model shall be performed to demonstrate the performance compared to Jónsdóttir's (2016) model. Jónsdóttir (2016) modelled the anchor-pipeline contact with CONT164. One of the observations from the simulations carried out so far is that numerical problems might occur for the contact element CONT164. The hypothesis is that CONT153 leads to less numerical problems than CONT164 for the anchor-pipeline interaction. A parametric study shall be performed to investigate how vessel velocity, pipe diameter, anchor size, span height, damping of the system, sloping seabed, seabed conditions, angle of attack between the anchor and the pipeline and water depth affect

the anchor-pipeline interaction. The pipeline is modelled as a ten-meter constrained rigid body in the parametric study. A global model shall be established to investigate how well the anchor's response is predicted in the parametric study.

Statoil defined the parameters that are of interest to investigate in the parametric study. The scope of the thesis is narrowed by only inspecting six different anchor sizes, two water depths, two pipe diameters and two towing velocities. The effect of angle of attack was only investigated for the case where the pipeline was resting on a flat seabed. Several of the models, where the angle of attack was not 90 degrees, were inconclusive. Less focus was therefore paid to the effect of angle of attack between the anchor and the pipeline in the parametric study.

1.4 Chapter overview

Chapter 2: *DNV GL rules and regulations* and chapter 3: *Literature review* cover the literature study. DNV GL rules and regulations, master theses and research papers of relevance will be presented. Chapter 4: *Non-linear finite element analysis* will give a brief introduction to non-linear finite element methods with particular focus on formulations used in SIMLA. Chapter 5 *Modelling* presents the SIMLA models for the hooking event. The contact elements are described in detail. Chapter 6: *Specifics of analyses* describe how the comparison study, the parametric study and the case studies are conducted. The results of the simulations are presented in chapter 6. The simulations, where CONT153 is used to model the anchor geometry and contact, are compared to Jónsdóttir (2016) results. The results of the parametric study and the case studies will also be discussed in chapter 6. The conclusion is presented in chapter 7 and suggestions to further work are discussed in chapter 8.

2 DNV GL rules and regulations

Currently, there is an ongoing project between DNV GL and Statoil to come out with a new recommended practice for anchor loads on pipelines. Four recommended practices and offshore standards from DNV GL of relevance to the topic anchor-pipeline interaction will be presented in this section. These practices and standards are related to design of pipelines, mooring and interference between trawling and pipelines.

2.1 DNV-OS-F101: Submarine pipeline systems

DNV-OS-F101 (2013) gives criteria and recommendations on concept development, design, construction, operation and abandonment of submarine pipeline systems.

Design loads

Section 4 in DNV-OS-F101 (2013) defines the loads to be checked by the limit states. The most critical load scenario shall be checked for all relevant phases and conditions. The loads are defined as either functional, environmental, interference or accidental.

- **Functional loads** arise due to the physical existence of the pipeline system.
- **Environmental loads** are loads on the pipeline system which are caused by the surrounding environment.
- **Interference loads** are imposed on the pipeline system from 3rd party activities. Typical interference loads are trawl interference, anchoring, vessel impacts and dropped objects.
- **Accidental loads** are imposed on a pipeline system under abnormal and unplanned conditions. The load is classified as an accidental load if the probability of occurrence is less than 10^{-2} within a year.

The probability of interference between dragging anchors and pipelines is less than 10^{-2} within a year, and it is therefore defined as an accidental load. Designing the structure against accidental loads may be performed:

- **Directly** by calculating the effects imposed by the loads on the pipeline.
- **Indirectly** by designing the pipeline as tolerable to accidents.

The design load effect for each limit state shall be checked. The load effect is defined as the resulting cross-sectional loads arising due to applied loads. The design load effect is defined as:

$$L_{Sd} = L_F\gamma_F\gamma_c + L_E\gamma_E + L_I\gamma_I\gamma_c + L_A\gamma_A\gamma_c \quad (1)$$

L_F is the load effect from functional loads, L_E is the load effect from environmental loads, L_I is the load effect from interference loads, L_A is the load effect from accidental loads, γ_F is the load effect factor for functional load, γ_E is the load effect factor for environmental

loads, γ_A is the load effect factor for accidental loads and γ_c is the condition load effect factor.

Design – limit state criteria

The Load and Resistance Factor Design (LRFD) is the basis for the design format in DNV-OS-F101 (2013). The design load effects (defined in equation 1) shall not exceed the design resistance for any of the considered failure modes in any load scenario. The design resistance is calculated by dividing the characteristic resistance by the resistance factors. The resistance factors depend on the pipelines safety class. The pipeline shall be classified into a low, medium, or high safety class reflecting the risk of human injury and environmental and economic consequences in case of failure.

The failure modes are divided into the following categories:

- **Serviceability Limit State (SLS):** The pipeline will be unsuitable for normal operation if this limit state is exceeded.
- **Ultimate Limit State (ULS):** The integrity of the pipeline will be compromised if this limit state is exceeded.
 - Fatigue Limit States (FLS): Accounts for accumulated cyclic load effects.
 - Accidental Limit State (ALS): Due to accidental (in-frequent) loads.

Table 3 lists the limit states (failure modes) that have to be considered in design of pipelines.

Table 3: Typical link between scenarios and limit states.

Scenario	Ultimate Limit States						Serviceability Limit States			
	Bursting	Fatigue	Fracture	Collapse	Propagating buckling	Combined loading	Dent	Ovalisation	Ratcheting	Displacement
Wall thickness design	X			X	X					
Installation		X	X	X	X	X		X		X
Riser	X	X	X	X	X	X		X		X
Free-span	(X)	X	X			X				
Trawling/3rd party	(X)	X				X	X			
On bottom stability	(X)	(X)	(X)			(X)	(X)	(X)		X ¹
Pipeline Walking		X				X				
Global Buckling	(X)	X	X			X			X	

1) Typically applied as a simplified way to avoid checking each relevant limit state

Which failure modes that have to be inspected for anchor loads are not specified in table 3. Loads from trawling/3rd party is the category that is most similar to anchor loads. The failure modes that must be investigated for trawling/3rd party are:

- **Bursting:** The pressure containment shall fulfill the following criteria:

$$p_{li} - p_e \leq Min \left(\frac{p_b(t_1)}{\gamma_m \gamma_{SC}}; \frac{p_{lt}}{\alpha_{spt}} - p_e; \frac{p_h \alpha_U}{\alpha_{mpt}} \right) \quad (2)$$

$$p_{li} - p_e \leq Min \left(\frac{p_b(t_1)}{\gamma_m \gamma_{SC}}; p_h \right) \quad (3)$$

where p_{li} is the local incidental pressure, p_e is the external pressure, p_b is the pressure containment resistance, p_h is the Mill test pressure, γ_m is the material resistance factor, γ_{SC} is the safety class resistance factor, α_{spt} is the system pressure test factor, α_u is the material strength factor and α_{mpt} is the Mill pressure test factor. The Mill pressure test is a hydrostatic test.

- **Combined loading criteria:** The DNV GL standard distinguishes between a load controlled condition (the structural response is primarily governed by the imposed loads) and a displacement controlled condition (the structural response is primarily governed by imposed geometric displacements). A condition is rarely pure load controlled or purely displacement controlled. Often the condition is an intermediate case. Different limit states apply to the two conditions, but a load controlled design criterion can always be applied in place of a displacement controlled design criterion. Pipe members subjected to bending moment, effective axial force and external overpressure shall be designed to satisfy the following criterion at all cross sections for the load controlled condition:

$$\left\{ \gamma_m \gamma_{SC} \frac{|M_{Sd}|}{\alpha_c M_p(t_2)} + \left\{ \frac{\gamma_m \gamma_{SC} S_{Sd}}{\alpha_c S_p(t_2)} \right\}^2 \right\}^2 + \left(\gamma_m \gamma_{SC} \frac{p_e - p_{min}}{p_c(t_2)} \right)^2 \leq 1 \quad (4)$$

where α_c is the flow stress parameter, M_{Sd} is the design moment, S_{Sd} is the design effective axial force, M_p denotes the plastic capacities for a pipe, p_c is the characteristic collapse pressure and p_{min} is the minimum internal pressure that can be sustained.

- **Dent** The maximum accepted dent depth is given by the following criterion:

$$H_p \leq 0.05\eta D \quad (5)$$

H_p is the permanent plastic dent depth, D is the nominal outside diameter and η is the usage factor.

- **Fatigue** The criterion for fatigue is given by:

$$D_{fat} DFF \leq 1 \quad (6)$$

$$D_{fat} = \sum_{i=1}^k \frac{n_i}{N_i} \quad (7)$$

where D_{fat} is the Miner's sum, k is the number of stress blocks, n_i is the number of stress cycles in stress block i , N_i is the number of cycles to failure at constant

stress range of magnitude $(\sigma_r)_i$ or strain range $(\epsilon_r)_i$, and DFF is the design fatigue factor.

2.2 DNV-RP-F111: Interference between trawl gear and pipelines

DNV GL does not have a standard for anchor-pipeline interaction, but there exists a standard for interference between trawl gear and pipelines. DNV-OS-F111 (2014) recommends conducting the pull over analysis as a dynamic analysis. It is uncertain whether neglecting inertia force is conservative or not. The global response will be reduced when inertia forces is accounted for, but inertia forces may cause localization of bending. The interference is divided into two phases:

- **Impact:** The initial impact phase which typically lasts some hundredths of a second. This will mainly give a local response of the pipeline.
- **Pull over:** The second phase which can last from one second to some ten seconds. This phase will mainly give a global response of the pipeline. Hooking is a seldom occurring situation in the pull over phase.

Design against impact requires assurance against the failure modes denting, collapse and fatigue. The loads and load effects are related to size, shape, velocity and mass of the trawling gear, and the standard can therefore only be used to calculate approximate loads and load effects caused by anchor-pipeline interactions.

2.3 DNV-RP-F107: Risk assessment of pipeline protection

DNV-RP-F107 (2010) provides a basis for risk assessment of accidental incidents which cause external interference with pipelines. Acceptance criteria, which states the acceptable limits for the risks to human safety, environment and economy, is used to evaluate whether the risk of an accidental event is acceptable or not. The frequency of occurrence and consequence of the end-events shall be evaluated to assess the risks. The evaluation can be based on calculations when detailed information exist, or it can be based on engineering judgment, operator experience, etc. The frequency of occurrence and the consequence are then given a ranking from 1 (i.e. low frequency/non-critical consequence) to 5 (i.e. high frequency/severe consequence). The total risk is evaluated by plotting the numbers in a risk matrix as shown in figure 1.

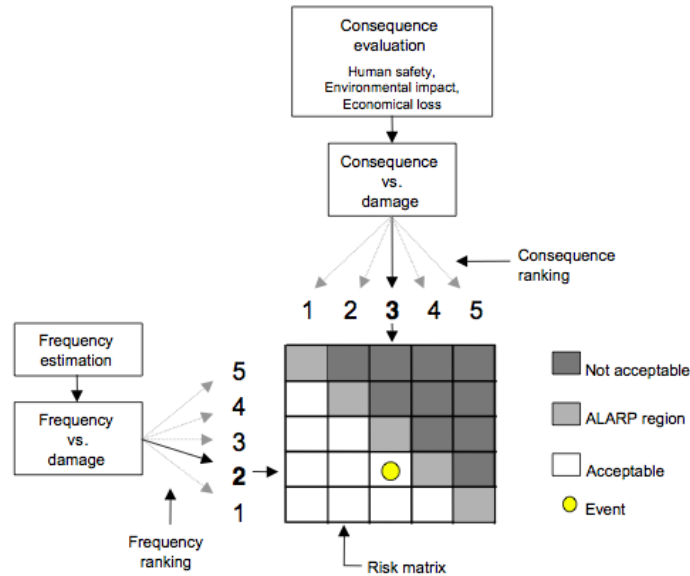


Figure 1: Process description of risk assessment (DNV-RP-F107, 2010)

ALARP is an abbreviation for as-low-as-reasonably-possible and this region is marked with light grey in figure 1. The risk in this area is acceptable, but risk reductions should be considered. The limits in figure 1 is only schematic, and the actual acceptance limits shall be given by the operator.

Impact due to dropped or dragged objects are typical accidental load scenarios that can damage pipelines. The response of an impact scenario is of a local nature and the wall thickness and coating thickness are important parameters. The recommend practice is to assume that the pipeline and coating absorb all the kinetic energy caused by the impacting objects if the energy absorption of the impacting object itself, or into the soil, is not well documented. The pull over and hooking scenario is of a global bending behavior. The capacity of the pipelines to withstand pull-over and hooking loads depends on the pipeline stiffness. The typical failure mode for impact loads are indentation or puncturing of the pipe wall and the typical failure mode for pull over and hooking loads are excessive bending. Local buckling is a result of excessive bending. Other relevant failure moods for pull over and hooking are covered in the criteria given in chapter 2.1. Increased ovalisation leading to collapse of the cross-section or rupture due to excessive yielding in the longitudinal direction may me the result if the criteria described in this chapter is exceeded. The failure modes will be further classified according to the damage (minor, moderate or major). Major damage is defined as damage leading to release of hydrocarbons or water. The damage categories are used for economic evaluations. The failure modes will be further classified (small release or major release) if the damage leads to release of fluids. The release categories are used for estimating the risk for human safety and leakage to the environment.

Anchor-pipeline interaction is rare, but the severity when it occurs could jeopardize the integrity of any pipeline. Vessels usually know where pipelines are located and avoid anchoring, but anchors might be dropped in emergencies and the drifting ship can represent a risk to subsea installations. Dropped anchors during emergency situations are usually a result of human error during the anchoring operation, failure of the chain braking system

or loss of the power supply to the chain braking system. Stand-by vessels can usually change the drifting course, and do not represent a significant risk to subsea installations. Drifting situations might occur for shuttle tankers, supply vessels and commercial ships. Shuttle tankers do typically have anchors with a mass of ten tones and the anchor mass for supply ship is typically two tones. A shuttle tanker has dynamic position system, the redundancy of the machinery is high and the loading of shuttle tankers is weather restricted. The risk of dragged anchors due to drifting of a shuttle tanker is therefore generally low. The frequency of emergency anchoring should be established for commercial shipping routes and the vessel size/class distribution should be established for the shipping lanes the pipeline is crossing. There is also a risk related to an anchor chain falling onto a pipeline or a drifting rig dragging an anchor over a pipeline. The breaking frequency per year per anchor is assumed to be 0.01. This assumption is based on known anchor breaking incidents for offshore rigs and production vessel up to 1993.

2.4 DNVGL-OS-E301: Position mooring

DNVGL-OS-E301 (2015) contains criteria, technical requirements and guidelines on design and construction of position mooring systems. Temporary mooring is considered in this thesis. Temporary mooring equipment shall be selected in accordance with the requirements given in table 4.

Table 4: Equipment table, (DNVGL-OS-E301, 2015)

Equipment number Exceeding – not exceeding	Equipment letter	Stockless anchors			Chain cables				
		Number	Mass per anchor (kg)	Total length (m) ²⁾	Diameter and grade				
					VL R3 or K3 ¹⁾	VL R3S	VL R4	VL R4S	VL R5
3 040 – 3 210	N	2	9 300	660	76	70	66	63	61
3 210 – 3 400	O	2	9 900	660	78	73	68	65	63
3 400 – 3 600	P	2	10 500	660	78	73	68	65	63
3 600 – 3 800	Q	2	11 100	687.5	81	76	70	67	65
3 800 – 4 000	R	2	11 700	687.5	84	78	73	69	67
4 000 – 4 200	S	2	12 300	687.5	87	81	76	72	70
4 200 – 4 400	T	2	12 900	715	87	81	76	72	70
4 400 – 4 600	U	2	13 500	715	90	84	78	74	72
4 600 – 4 800	V	2	14 100	715	92	87	81	77	75
4 800 – 5 000	W	2	14 700	742.5	95	90	84	80	78
5 000 – 5 200	X	2	15 400	742.5	97	90	84	80	78
5 200 – 5 500	Y	2	16 100	742.5	97	90	84	80	78

The required anchor mass, chain length and diameter for a given equipment number is presented in table 4. The equipment number (row 1 in table 4) is given by:

$$EN = \Delta^{2/3} + A \quad (8)$$

where Δ is the moulded displacement in salt waters on maximum transit draught and A is the projected area of all the wind exposed surfaces above the unit's light transit draught, in an upright condition, taken as the projection of the unit in a plane normal to the wind direction.

3 Literature review

3.1 Research papers

The research on anchor-pipeline interaction is quite limited. However, some studies on dropped and dragged anchors are conducted. Research papers on dragging anchors interacting with pipelines will be presented in this section. All papers presented are published in the International Ocean and Polar Engineering Conference. This master thesis is about dragging anchors, and only papers related to this topic will be presented in this chapter. The studies on the subject anchor-pipeline interactions primarily focus on the potential damage anchor may inflict on a pipeline, the replacement length when accidents happen and risk studies.

Sriskandarajah and Wilkins (2002) presents an assessment of anchor loads on pipelines and the potential damage an anchor may inflict on a pipeline. The paper investigates incidents where the anchor is dragged onto a pipeline either resting on a continuous seabed or partially buried in the seabed. The response of the pipeline was determined by performing a dynamic non-linear finite element analysis. The anchor forces of interest, according to Sriskandarajah and Wilkins (2002), are the force at which pipeline movement is initiated, the forces at which a pipeline reaches its maximum allowable design stress and the force at which the pipeline buckles. A pipeline of 10 km is modeled and analyzed in Abaqus. The results of the research is showed in tables 5 and 6. The outer diameter of the pipeline is not specified in the paper.

Table 5: Lateral force limits for pipeline resting on a seabed (Sriskandarajah and Wilkins, 2002)

Pipeline design limit	Lateral force (kN)
1 m lateral displacement	73
Design stress limit	150
Onset of lateral buckling	525

Table 6: Lateral force limits for pipeline partially buried (Sriskandarajah and Wilkins, 2002)

Pipeline design limit	Lateral force (kN)
0.2 m lateral displacement	400
Design stress limit	420
Onset of lateral buckling	575

Al-Warthan et al. (1993) analyzed, by a discrete element method, the static and dynamic deflections, and the axial and bending stresses on three different span lengths of a free span pipeline. Three loading functions were considered: triangular impulse loading, ramp loading and hook loading. An impulse loading represents the direct impact force on a pipe. The analyzes showed that the maximum stresses, for all span lengths, occurred for the ramp loading. The study also showed that the stresses increased as the span length decreased. Al-Warthan et al. (1993) concluded that an offshore pipeline could fail

due to anchor impacts. Protective means should therefore be incorporated when offshore pipelines are being designed.

Impact loading and hooking are the two accidental loading scenarios that are generally considered when it comes to serious damage of a pipeline. Impact loading is usually due to dropped anchors while hooking is caused by dragged anchors or trawl boards. Oosterkamp et al. (2013) considered the hooking scenario. A 42" gas pipeline with a wall thickness of 34 mm is being dragged by an anchor. The large bending deformation combined with a large local force caused by the dragging anchor leads to rupture of the pipeline. The production must be stopped instantly when the pipeline ruptures to reduce the consequences, and required repair must be performed. Rupture of pipelines cause serious environmental pollution and economical loss. The downtime would be reduced if the pipe's damaged length is known in advance. Oosterkamp et al. (2013) developed a modeling approach to predict the replacement length based upon a case study. The analyses comprise of three main steps. The flow condition inside the pipeline and the fluid interaction with the pipeline is calculated in the first step. The calculations in this step are performed using OLGA, which is a one-dimensional pipe flow simulation tool. The mechanical response of the pipeline due to the imposed load from the anchor is determined in the second step. Finite element analysis is used to study the pipelines reaction from impact until rupture. The position where local buckling of the pipeline occurs and whether the pipeline collapses is identified in step three. Both step two and three are performed in ANSYS.

Risk studies are carried out to analyze the potential anchor damage on offshore pipelines. The studies give valuable information on minimum burial depth and protection cover requirements. Hvam et al. (1990) studied the risk of both dropped and dragged anchors. The risk studies encompass:

- **Anchor-pipeline interaction frequency:** This is found from ship traffic data from the concerned area, failure rates and data regarding procedures under emergency conditions.
- **Capacity of the pipeline to tackle localization impacts and hooking loads:** Kinetic energy is assumed to be fully transferred to the pipe when the anchor hits the pipeline. This is in accordance with DNV-RP-F107 (2010). It is assumed that the pipe is able to absorb all the initial impact energy and the pipe will not experience permanent deflection. The concrete coating will generally break in this first impact. A point load is applied to the pipeline if the anchor is able to hook the pipeline. The pipeline will then deflect as a beam, but it is hindered by the soil reaction. The pipeline will get a dent if the hooking force is large.
- **Risk of damage:** The anchor-pipeline interaction frequency and the capacity of the pipeline to tackle localization impacts and hooking loads is the basis for calculation of the cumulative probability of failure. Protection measures, like burial depth or protection cover, must be introduced if the failure probability exceeds the acceptance criterion.

3.2 Geometrical consideration of the anchor hooking problem

The old fashion Hall and SPEK type anchors, specially designed to fit anchor pockets, are the most common conventional anchor for most ships according to anchor manufacturer SOTRA (SOTRA, 2014a). The Spek type anchor was utilized by Wei (2015) and Jónsdóttir (2016) in their master theses and this anchor type will be utilized in this master thesis as well. The geometry of the Spek type anchor is illustrated in figure 2 and the dimensions for anchors with different masses are listed in table 7.

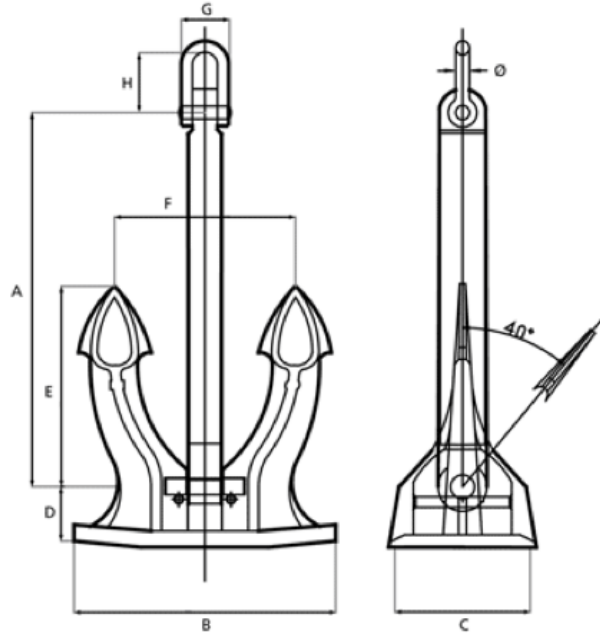


Figure 2: Spek anchor (SOTRA, 2014a)

Table 7: Dimensions (figure 2) for different anchor masses (SOTRA, 2014a)

Mass [kg]	A [mm]	B [mm]	C [mm]	D [mm]	E [mm]	F [mm]	G [mm]	H [mm]	Ø [mm]
3780	2430	1850	810	393	1350	1350	3100	385	90
4890	2520	1926	852	413	1400	1400	346	415	100
6000	2700	2060	900	446	1500	1500	350	450	100
7800	2920	2138	930	456	1550	1550	380	500	110
9900	3160	2332	1020	510	1700	1700	421	580	124
15400	3690	2824	1230	615	2050	2050	498	680	150

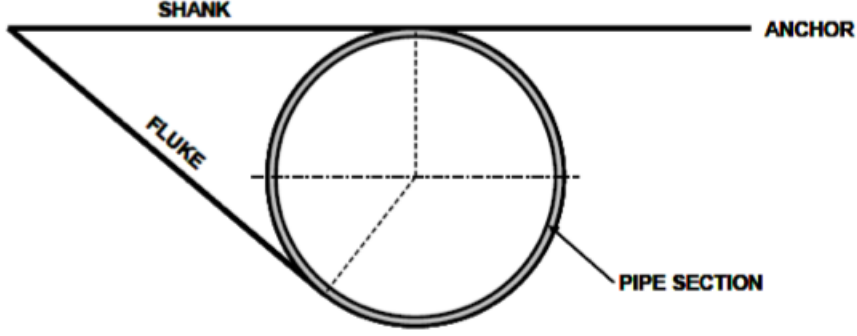


Figure 3: Hooked pipe section (Nord Stream, 2008)

A pure geometrical consideration of the anchor-pipeline interaction problem has been performed by Nord Stream (2008). The maximum pipe diameter an anchor can hook onto is:

$$D_{max} = \frac{2L(1 - \cos\alpha)}{\sin\alpha} \quad (9)$$

L is the fluke's length and α is the angle between the fluke and the shank. It is assumed that the anchor flukes and shank do not have any significant width. This assumption is valid for the anchor flukes, but the anchor shank does have a significant width. The maximum diameter the anchor can hook onto will be slightly reduced compared to the pipe diameter calculated in equation 9. A modified fluke's length is therefore used to calculate the maximum diameter an anchor can hook onto. $L_{modified}$ is calculated as $L - \Delta L$. ΔL is calculated by dividing the shank width by $\sin(40)$. The width of the shank is not presented in table 7. The shank width is assumed to be $1/7$ of the length c given in figure 2. The maximum calculated hooking diameter, D_{max} , for various anchor sizes of the Spek anchor is presented in table 8.

Table 8: Maximum hooking diameter for Spek anchors

Anchor weight [Kg]	Fluke angle [deg]	E [mm]	Delta L [mm]	L modified [mm]	C [mm]	Shank width [mm]	D_{max} [mm]
3780	40	1350	180	1170	810	115.7	851.7
4890	40	1400	189.3	1210.7	852	121.7	881.3
6000	40	1500	200.0	1300.0	900	128.6	946.3
7800	40	1550	206.7	1343.3	930	132.9	977.9
9900	40	1700	217.3	1482.7	1020	139.7	1079.3
15400	40	2050	273.4	1776.6	1230	175.7	1293.3

This mathematical model does only consider the anchor and pipeline geometry. Effects like seabed conditions, towing speed, water depth, directionality etc. are not considered.

3.3 Master theses

Three master theses have previously been written at the institute of marine technology at NTNU related to the subject anchor loads on pipelines. Vervik’s master thesis (2011) is based on the anchor hooking incident at the Kvitebjørn Gas Pipeline. Wei (2015) and Jónsdóttir (2016) focused on numerical simulation of the anchor hooking event in SIMLA. This project thesis is a continuation of this work.

3.3.1 Pipeline accidental load analysis

Vervik (2011) investigated which circumstances, in terms of vessel velocity, anchor mass, pipe diameter, chain length versus water depth and chain breaking strength, that must be fulfilled in order for the anchor to hook onto the pipeline. He used the model developed by Nord Stream to evaluate whether the anchor was large enough so that a pipeline could get stuck between the anchor shank and flukes. This model is described in section 3.2. He also investigated the probability of a vessel, that meets these requirements, passing the Kvitebjørn gas pipeline. He then developed a SIMLA model to predict pipeline response and strains when an anchor hooks a pipeline. The anchor sizes and associated chain parameters presented in table 9 formed the basis for the evaluation of the anchor interaction with the Kvitebjørn gas pipeline.

Table 9: Equipment letter parameters. A variety of anchor sizes and the associated chain parameters. (Vervik, 2011)

Equipment letter	Chain length [m]	Chain diameter [mm]	Grade	Anchor mass [kg]	Chain strength [kN]
z	522,5	48	K3	3780	1810
G	577,5	60	K3	6000	2770
L	632,5	70	K3	8300	3690
O	660,0	78	K3	9900	4500
X	742,5	97	K3	25400	6690
A*	742,5	102	K3	17800	7320
E*	770,0	117	K3	23000	9300

The anchors are divided into six classes based on their equipment number.

Table 10: Anchor classes (Vervik, 2011)

Anchor class	Equipment letter	Anchor mass [kg]
Class 1	z-G	3780 – 6000
Class 2	G-L	6000 – 8300
Class 3	L-O	8300 – 9900
Class 4	O-X	9900 – 15400
Class 5	X-A*	15400 – 17800
Class 6	A*-E*	17800 – 23000

Vervik (2011) studied historical ship data in order to determine the number of cargo ships, tankers and tug vessels passing the Kvitebjørn pipeline every year. The total number of

ships passing the pipeline between March 2010 and March 2011 was 7160. 58 % of the ships had anchors with dimensions large enough to hook onto the pipeline. Class 1 may be seen as a lower limit for anchor hooking to happen. Vervik (2011) calculated the maximum tow depth for each anchor class for vessel velocities between 2 and 17 knots. When all these parameters are considered, only 237 out of 7160 (3,3%) anchors could hook onto the pipeline. Ship headings when crossing the pipeline sections were not investigated. The distribution of anchor classes for these 237 vessels able to hook the pipeline is shown in Figure 4.

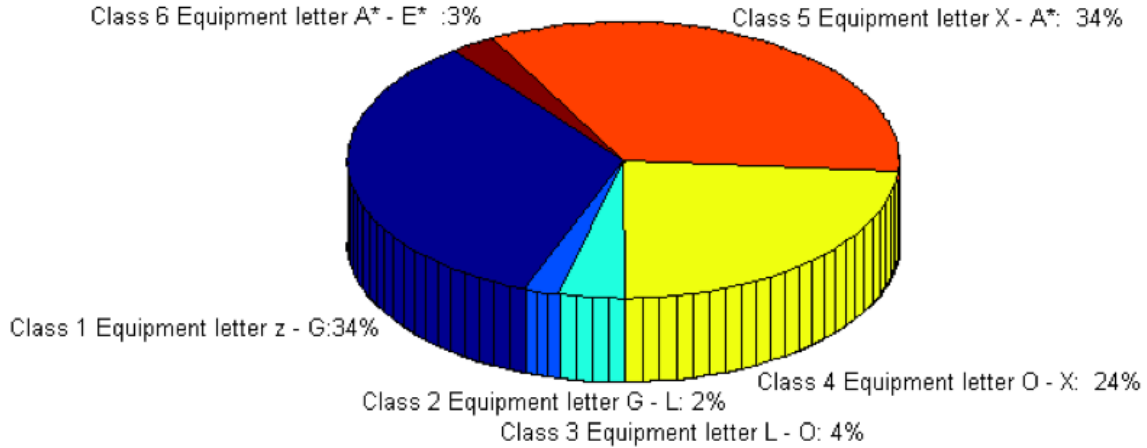


Figure 4: The distribution of anchor classes for the vessels able to hook the Kvitebjørn pipeline.

The ship traffic is largest over pipeline sections located at water depths of approximately 300 meters. Only anchors of class 3 or above are able to touch down to the seabed at this depth.

3.3.2 Anchor loads on pipelines

Wei (2015) focused on numerical simulation of the anchor hooking event in SIMLA. She investigated which parameters that would increase the probability of hooking. The SO-TRAs Spek anchor's dimensions were the basis for the anchor model. The pipeline was modeled as a ten-meter constrained rigid body. This short pipe model made it possible to run a large number of analysis. The parameters Wei (2015) investigated were pipe diameter, span height, anchor mass, hooking angle and vessel velocity. Table 11 shows the values used for the different parameters.

Table 11: Parameters inspected by Wei (2015)

Anchor mass [kg]	Pipe Diameter [m]	Hooking Angle [°]	$\frac{Spanheight}{Diameter}$ [-]
3780	0.4	90	0
6000	0.6	100	1
9900	0.8	110	2
15400	1.0	120	3

Wei (2015) concluded that the hooking ratio increases with increasing anchor mass. Reducing the pipe diameter or the vessel velocity increased the hooking ratio. Larger span heights reduce the probability of hooking. The hooking ratio decreased with increasing hooking angle.

Four "long pipeline" models were established to investigate the pipeline response until the anchor chain failed. The investigation showed that the anchor cable force increases approximately linearly during the hooking event until the cable reaches the capacity limit.

3.3.3 Simulation of anchor loads on pipelines

Jónsdóttir (2016) studied the anchor's and the pipeline's response to anchor-pipeline interactions. Three different studies were carried out to investigate this interaction. The first study investigated how different parameters, such as anchor size and vessel velocity, affected the anchor's response when it collided with a pipeline. The second analysis determined the minimum chain length that would cause anchor-pipeline interaction when the anchor was towed at 2 and 10 knots. The third and final analysis investigate the global response of the pipeline when exposed to anchor forces. The water depth was 200 meters for all analyses.

A parametric study was conducted to investigate the effect of anchor mass, anchor geometry, pipe diameter, vessel velocity and angle of attack on the anchor's response. The values used for the different variables are shown in Table 12.

Table 12: Parameters investigated by Jónsdóttir (2016)

Anchor Mass [kg]	Anchor Length [m]	Anchor Chain	Pipe Diameter [inches]	Vessel velocity [knots]	Angle of Attack [deg]
3780	Z	522.5	30	2	90
4890	D	550	40	10	60
6000	G	577.5			30
7800	K	632.5			
9900	O	660			
15400	X	742.5			

SIMLA models for the hooking event that allowed for sliding under friction along the pipeline were established. The pipeline was modelled as a 10-meter-long constrained rigid body. The anchor chain length was set equal to the maximum anchor chain length recommended by DNV GL for the respectable anchor mass. The response of the anchor was categorized as brief or lasting contact. Brief contact was defined as either pull over or bounce over and lasting contact was either defined as hooking or sliding, with or without twisting. Table 13 shows how the angle of attack between the anchor and the pipeline, pipe diameter, vessel velocity and anchor mass affect the hooking ratio. None of the models hooked onto the pipeline when the angle of attack between the anchor and the pipeline was 30 degrees.

Table 13: Hooking ratio distribution (Jónsdóttir, 2016)

Angel of attack [degrees]	Pipe diameter [inches]	Vessel velocity [knots]	Anchor mass [kg]						Sum
			3780	4890	6000	7800	9900	15400	
90	30	2						10 %	10 %
		10			10 %			10 %	20 %
60	30	2			10 %	10 %	10 %	10 %	40 %
		10						10 %	10 %
60	40	2						10 %	10 %
		10						10 %	10 %
		Sum			10 %	20 %	10 %	60 %	100 %

Jónsdóttir (2016) concluded that the hooking ratio increased with increasing anchor size, decreasing pipe diameter and decreasing vessel velocity. This is in accord with Wei's (2015) results. The parametric study showed that the pipeline is more prone to anchor hooking when the angle of attack is 60 degrees than when the angle is 30 or 90 degrees. The contact between the anchor and the pipeline was modeled with the contact element CONT164. One of the observations from the simulations carried out were that numerical problems might occur for the contact element CONT164. In addition to the numerical problems did several simulations show unrealistic responses when the anchor collided with the pipeline. A simulation was said to be unrealistic if the anchor pierced the pipeline, or if the anchor grossly deformed. Table 14 shows which models that experienced realistic, non-realistic and inconclusive responses.

Table 14: Overview of results in the parametric study (Jónsdóttir, 2016)

	Anchor mass [kg]					
	3870	4890	6000	7800	9900	15400
Realistic	1	2	6	7	8	12
Unrealistic	11	9	3	3	1	0
Inconclusive	0	1	3	2	2	0

Table 15 shows the minimum required anchor chain length for different anchor masses and vessel velocities.

Table 15: Minimum required anchor chain length (Jónsdóttir, 2016)

Minimum length [m]	Anchor mass [kg]					
	3870	4890	6000	7800	9900	15400
2 knot	203.62	203.24	202.94	202.58	202.26	201.74
10 knot	321.05	318.11	315.58	301.62	309.06	302.56

The pipeline's global response was analyzed in the third study. Eleven case studies were conducted. The pipeline was modeled as ten-kilometer-long, with elastoplastic material properties and constrained ends. Less than 30 % of the case studies resulted in hooking. No hooking response was observed in the case studies when the angle of attack between the anchor and the pipeline was 60 degrees. Jónsdóttir concluded that the rigid modelling of the pipeline, rather than the anchor's response, caused the hooking response in the parametric study.

4 Non-linear finite element analysis

The finite element method is an approximate numerical analysis procedure used to solve a wide variety of problems like structural analysis, fluid flow and heat transfer. The finite element method discretizes the model into a finite number of subsystems known as elements. The relation between the element forces and the displacement for each element is calculated. The stiffness matrices for all elements are assembled into the global stiffness matrix. The system displacements are calculated and the element forces can be found from the relation:

$$\mathbf{S} = \mathbf{k}\mathbf{v} \quad (10)$$

\mathbf{k} is the element stiffness matrix and \mathbf{v} is the end-point displacement vector (Moan, 2003).

SIMLA is a finite element based program for non-linear static and dynamic analysis of pipelines. The software tool simulates the structural response of a pipe and allows inspection of the result by 3D graphical visualization. SIMLA is developed by Norwegian Marine Technology (MARINTEK). This section will review non-linear finite element theory with focus on the formulations used in SIMLA.

4.1 Basic principles of structural analysis

Structural analysis is based on the following principles:

- Equilibrium (expressed by stresses)
- Kinematic compatibility (expressed by strains)
- Material law (expressed by stress-strain relationship)

4.1.1 Equilibrium

The exact solution of a structural problem requires that equilibrium is achieved for every part of the structure. The differential equation may be unsolvable in many cases. The solution of the equilibrium equation must therefore be approximated (Moan, 2003). The principle of virtual displacement is applied in SIMLA to obtain an approximate solution of the equilibrium equation. The principle of virtual displacement states : «The total virtual work performed by a system in equilibrium when it is subjected to virtual compatible displacements is equal to zero.» (Langen and Sigbjörnsson, 1986, p. 3.1). Volume forces are excluded in SIMLA, but initial stresses are accounted for (Sævik, 2008).

4.1.2 Kinematic compatibility

The completeness criterion and the compatibility criterion must be satisfied to ensure that the finite element solution converges to the exact solution. The completeness criterion requires that the element represents all rigid body modes and all constant strain modes. The compatibility criterion states that the displacements and the derivatives through order $m - 1$ must be continuous across the boundaries between elements. m defines the order

of the strain-displacement differential operator (Moan, 2003). The strain is expressed as the Green strain tensor, which is found to be:

$$E_{xx} = u_{x0,x} - yu_{y0,xx} - zu_{z0,xx} + \frac{1}{2}(u_{y0,x}^2 + u_{z0,x}^2) + \theta_{,x}(yu_{z0,x} - zu_{y0,x}) + \frac{1}{2}\theta_{,x}^2(y^2 + z^2) \quad (11)$$

$$u_x(x, y, z) = u_{x0} - yu_{y0,x} - zu_{z0,x} \quad (12)$$

$$u_y(x, z, y) = u_{y0} - z\theta_x \quad (13)$$

$$u_z(x, y, z) = u_{z0} - y\theta_x \quad (14)$$

where θ_x is the rotation about the x-axis and u is the displacement. The second order longitudinal strain term in the Green strain tensor, the coupling terms between longitudinal strain and torsion and shear deformations are neglected (Sævik, 2008). Green strains are based on the 'square' of the length, and 2nd Piola-Kirchhoff stresses should be applied if Green strains are used. The 2nd Piola-Kirchhoff stress is referred to the initial configuration of the structure. Green strain is widely used in problems with geometric non-linearity (Moan, 2003).

4.1.3 Material law

Hook's law expresses the relation between stresses and strains for an elastic material:

$$\begin{bmatrix} \sigma_{11} \\ \sigma_{22} \\ \tau \end{bmatrix} = \frac{E}{1 - \nu^2} = \begin{bmatrix} 1 & \nu & 0 \\ \nu & 1 & 0 \\ 0 & 0 & \frac{1-\nu^2}{2(1+\nu)} \end{bmatrix} = \begin{bmatrix} \epsilon_{11} \\ \epsilon_{22} \\ \gamma \end{bmatrix} \quad (15)$$

where ϵ_{11} and ϵ_{22} are the principal strains, σ_{11} and σ_{22} are the principal stresses, E is the modulus of elasticity and ν is the Poisson's ratio.

An elastoplastic material model is required if the stresses exceed the elastic limit (yield strength). The strain increment is composed of one elastic and one plastic contribution when yielding has occurred (Moan, 2003).

$$d\epsilon = d\epsilon^e + d\epsilon^p \quad (16)$$

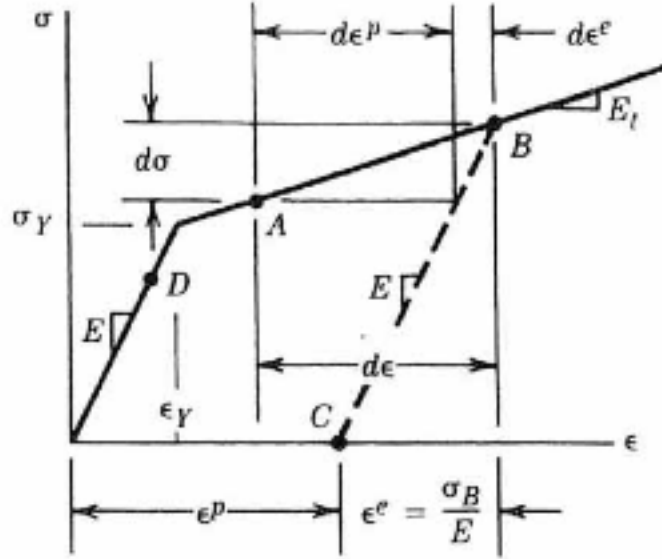


Figure 5: Stress-strain relationship. σ_y is the stress at the first onset of yielding (Moan, 2003)

Three basic principles govern the elastoplastic material behaviour:

- **The yield criterion:** Yielding starts when the stress $|\sigma|$ reaches σ_y . σ_y is usually taken as the tensile yield strength. The material starts to deform plastically when the stress reaches the yield stress (Moan, 2003). The yield condition is expressed as:

$$f(\mathbf{S}, \kappa) = 0 \quad (17)$$

where f is a scalar function, κ is a strain-hardening parameter which is dependent of the load history in the plastic range and \mathbf{S} is the stress tensor of 2nd Piola-Kirchhoff stress. Equation 17 is assumed to describe a closed surface called a yield surface. The surface is in a six-dimensional stress space. Equation 18 is called the consistency condition and it prevents stresses from exceeding the yield limit. (Sævik, 2008)

$$f = \frac{\partial f}{\partial \mathbf{S}} : \dot{\mathbf{S}} + \frac{\partial f}{\partial \kappa} \dot{\kappa} \quad (18)$$

- **A hardening rule:** Describes how the history of plastic flow changes the yield criterion. The hardening rules included in the material model in SIMLA are kinematic and isotropic hardening (Sævik, 2008). Isotropic hardening means that the yield surface remains the same shape but expands with increasing stress. Kinematic hardening means that the yield surface remains the same shape and size. The yield surface merely translates in the stress space (Kelly, 2012). The kinematic hardening rule is the best match to the observed behaviour of common metals (Moan, 2003).
- **A flow rule:** Is needed in order to relate the stress increments to the strain increments.

4.2 Non-linear effects

Linear theory is based on the assumptions that displacements are small and that the material is linear elastic. These assumptions need to be modified when the ultimate strength of structures that buckle and collapse is to be calculated. We need to account for:

- Geometrical nonlinear behaviour
- Material nonlinear behaviour
- Boundary non-linearity

Geometrical non-linear behavior is accounted for when establishing the equilibrium equations. Material non-linear behavior is associated with nonlinear stress-strain relationship. Boundary non-linearity must be accounted for when surfaces come into or out of contact. The applied loads are in most cases not linearly dependent on the displacements and stresses of the contacting bodies. Non-linear structural analysis must be performed on contact problems even if the displacements are small and the material behavior is linear since the contact area is usually not linearly dependent on the applied loads. When two surfaces come into contact slick-slip behavior may occur. This is an effect caused by friction and it adds a further non-linear complexity to the problem. (Moan, 2003)

4.3 Solution methods

4.3.1 Static solution

A static analysis is conducted to ensure that the system is in equilibrium before the onset of the dynamic load. The static problem is expressed as:

$$\mathbf{K}\mathbf{r} = \mathbf{R} \quad (19)$$

\mathbf{K} is the stiffness matrix, \mathbf{r} is the displacement vector and \mathbf{R} is the load vector. The Newton-Raphson method is used to solve static problems in SIMLA. The Newton-Raphson method is an iterative method. This method requires that the stiffness matrix is updated in each iterative step and that iterations are repeated until convergence has been obtained. A predefined number of interactions will be performed in SIMLA. The time step will be divided and a new trial will be initiated if equilibrium is not achieved. (Sævik, 2008)

$$\mathbf{r}_{n+1} - \mathbf{r}_n = \Delta\mathbf{r}_{n+1} = \mathbf{K}_I^{-1}(\mathbf{r}_n)(\mathbf{R} - \mathbf{R}_{int}) \quad (20)$$

$$\mathbf{r}_{k+1} = \mathbf{r}_k + \Delta\mathbf{r}_{k+1} \quad (21)$$

4.3.2 Dynamic solution

A dynamic analysis must be performed since the anchor's impact on the pipeline is a dynamic load. It is also recommended in DNV-OS-F111 (2014) to conduct the pull over analysis as a dynamic analysis. The dynamic problem is expressed as:

$$\mathbf{M}\ddot{\mathbf{r}} + \mathbf{C}\dot{\mathbf{r}} + \mathbf{K}\mathbf{r} = \mathbf{Q} \quad (22)$$

\mathbf{M} denotes the mass matrix, \mathbf{C} is the damping matrix, \mathbf{K} is the stiffness matrix, \mathbf{Q} is the load vector and \mathbf{r} is the displacement vector.

Dynamic nonlinear problems are solved by a direct time integration of the equation of motion. The time integration can either be performed by an explicit method or an implicit method. The method is explicit if the displacements at the new time step is expressed by the displacements, velocities and accelerations of previous time steps. Explicit methods are conditionally stable. This means that the numerical stability is dependent on the size of the time step. Small time steps must therefore be used. Implicit methods obtain the displacements at the new time step from the velocities and accelerations at the new time step and by historical information at previous time steps. Implicit methodologies require computer capacity in terms of memory resources (Moan, 2003). Implicit methods have better numerical stability than explicit methods since implicit methods use information at the next time step (Sævik, 2008). The difference between the implicit methods lie in the assumptions which are made related to how the acceleration is assumed to vary between the time steps. The method will be unconditionally stable if constant average acceleration is assumed between the time steps. Numerical stability is provided regardless of the time step size if the method is unconditionally stable (Sævik, 2008). This method will therefore be beneficial to use if the duration of the analysis is long. An implicit solution method is used for the simulations of the anchor-pipeline interaction in SIMLA.

4.4 Finite element formulation

A reference system for describing the geometry and the deformations of the system must be chosen when the non-linear geometrical problem is formulated. The two most common reference systems in structural mechanics are the Total Lagrangian and the Updated Lagrangian formulations. The Total Lagrangian formulation is based on a fixed coordinate system. All deformations are referred to the initial configuration. The updated Lagrangian formulation is based on local coordinate systems that are updated as the structure deforms. The static and kinematic variables are referred back to the updated coordinate systems (Moan, 2003). The co-rotational formulation, which is a combination of the two formulations mentioned earlier, is applied in SIMLA. The co-rotational formulation separates the rigid body motion from the local deformation of the element. A local element system is fixed to the element and the coordinate system is updated as the element deforms. All quantities are referred to the initial configuration when the co-rotated formulation is applied (Sævik, 2008).

5 Modelling

This chapter describes the modelling of the anchor-pipeline interaction. The model consists of a pipeline, an anchor, an anchor chain, seabed, sea surface, environmental conditions and contact elements. The model is shown in figure 6.

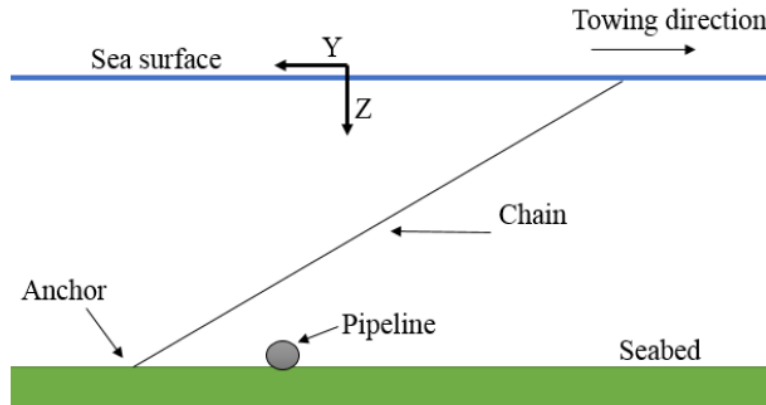


Figure 6: Model of the anchor-pipeline interaction (Jónsdóttir, 2016)

The analyses of the anchor-pipeline interactions are carried out by applying the computer tool SIMLA. An input file, prefix.sif, is run by SIMLA. An output file .sof, a log file .slf and a results database .raf and .dyn are created. Xpost creates a visual presentation of the results from the .raf file.

5.1 Pipe elements

The pipeline and chain were modelled with pipe elements. Figure 7 shows the degrees of freedom for a pipe element.

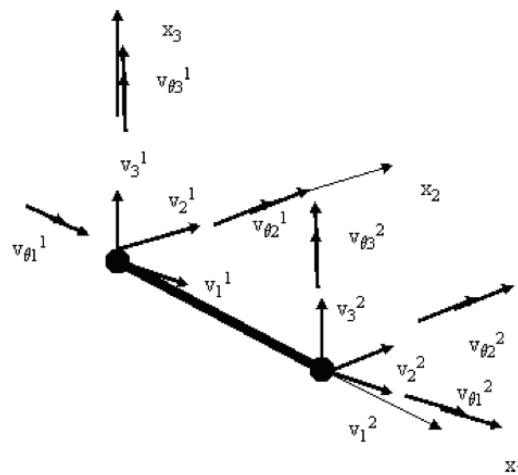


Figure 7: Degrees of freedom for a pipe element (Sævik, 2008)

A pipe element is modelled with two nodes. Each node has six beam degrees of freedom; three translations and three rotations. Loads include linear interpolated loads along the elements and hydrodynamic loads. The loads along the elements are analytically calculated and the hydrodynamic loads are found using Morison’s equation. The damping for pipe elements include lumped and Rayleigh damping (Sævik, 2008). The Rayleigh damping matrix is defined as:

$$\mathbf{C} = \alpha_1 \mathbf{M} + \alpha_2 \mathbf{K} \quad (23)$$

\mathbf{M} is the mass matrix, \mathbf{K} is the stiffness matrix and α_1 and α_2 are constants of proportionality.

The material model and the kinematic relations differ for different pipe elements. PIPE31 has an elastic material model. Plane stress is assumed, and the element has therefore only two normal stress components and one shear component. Coupling terms between longitudinal strain and torsion and shear deformations are neglected. PIPE33 has an elastoplastic material model and the element accounts for both stresses in the axial and the hoop directions. Coupling terms between longitudinal strain and torsion is accounted for, whereas shear deformations are still neglected.(Sævik, 2008)

5.1.1 Pipeline

The pipeline was modelled as a ten meter long rigid body in the parametric study. The pipeline was constrained against all displacements. PIPE31 elements were chosen since the main purpose of this study was to investigate the anchor’s behaviour. The MATLAB function calculating the distributed weight of the pipe and the submerged weight was received from Jónsdóttir (2016). The important parameters for the pipeline are listed in table 16.

Table 16: Important pipeline parameters

Property	Value	Unit
Density steel	7850	kg/m ³
Density asphalt	1300	kg/m ³
Density concrete	2500	kg/m ³
Density content	800	kg/m ³
Thickness asphalt layer	6	mm
Thickness concrete layer	45	mm
Total outer diameter (30-inch)	864	mm
Toryal outer diameter (40-inch)	1118	mm

The pipeline was modelled as ten kilometer long in the elastoplastic case studies. This made it possible to inspect the actual response of the pipeline. PIPE33 elements were chosen to model the pipeline. The pipeline was only constrained at the end nodes. The ends of the pipeline were connected to spring elements. The pipeline was allowed to globally deform. The boundary conditions for the pipeline end nodes and the spring are described in table 17.

Table 17: Boundary conditions for the pipeline

	Pipeline end nodes	Spring
Translation in x-direction	free	fixed
Translation in y-direction	fixed	fixed
Translation in z-direction	free	fixed
Rotation about x-axis	fixed	fixed
Rotation about y-axis	free	fixed
Rotation about z-axis	free	fixed

5.1.2 Chain

Mooring lines can be made of synthetic fiber ropes, steel ropes or chains. Chains are divided into stud link chain cable or studless link chain cable. A stud link chain has a stud across its middle. This gives the chain extra rigidity and the stud link chain has therefore higher strength than the studless chain. Figure 8 shows a stud link chain.

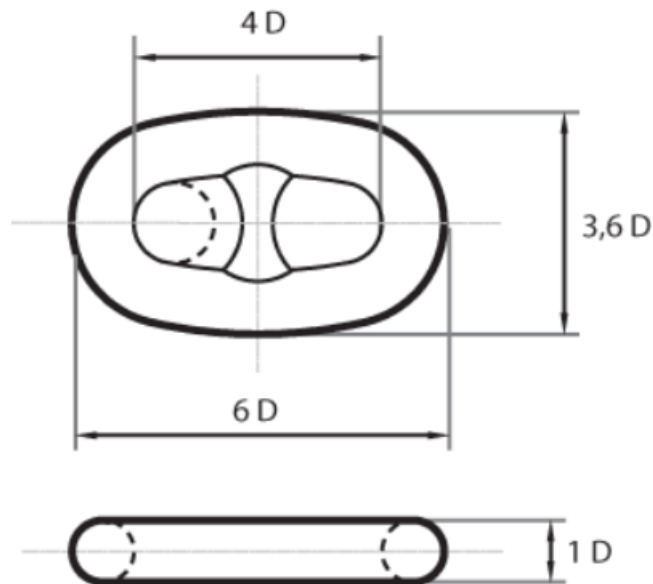


Figure 8: Stud Link Chain (SOTRA, 2014b)

The chain was designed according to the requirements given by DNV GL. The chain was modelled with 1000 PIPE31 elements. The geometry was simplified by modelling the chain's cross-section circular. The diameter was set to four times the chain diameter given in table 4. The calculations related to the anchor chain are taken directly from Jónsdóttir (2016). The drag coefficients for chain were found to be 2.6 in transverse direction and 1.4 longitudinal direction (Jónsdóttir, 2016).

5.2 Anchor

A three-dimensional mesh of geometry elements modelled the anchor. The shank was modelled as a cylinder, while the flukes were modelled as either circular or elliptic cylinders. The radius of the circles/ellipses decrease toward the tip of the fluke creating a pointed end at the tip. The area where the flukes and shank are connected was not modelled since this part of the anchor would not come into contact with the pipeline. Figure 9 shows the anchor models.

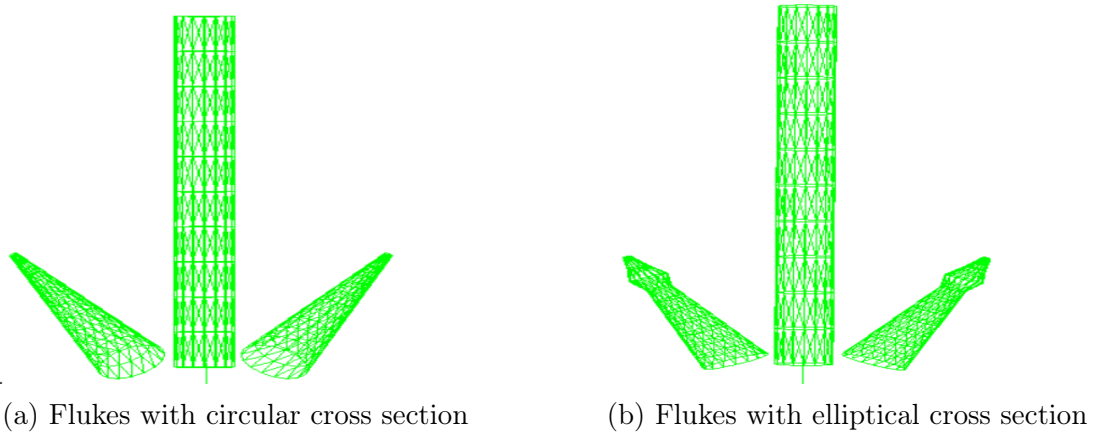


Figure 9: Anchor models

The node positions and the topology matrix were calculated in the MATLAB function `AnchorGeometry.m` and the 3D geometry description was stored in the file `AnchorGeometry.dat`. The file `AnchorGeometry.dat` starts with one line with three numbers: the number of elements, the number of element nodes and the number of nodes in the model. Only triangular elements are allowed when `CONT153` is used. Line two defines the radius of side edges and corners of the geometry. Then comes the topology and at last the xyz coordinates. The anchor geometry is connected to `BODY502`, which is a one noded element. The `GEOM` card is applied to specify a geometry for an element of type body. The geometry is connected to the body element, but the anchor load, mass and damping are connected to pipe elements.

5.3 Soil

5.3.1 Material curve in y-direction

The American Petroleum Institute (API RP2A 93) proposed the following empirical material curve for sand:

$$p = Ap_u \tanh\left(\frac{kXy}{Ap_u}\right) \quad (24)$$

where k is the initial modulus of subgrade reaction which is determined from the graph given in figure F-5 in DNV-OS-J101 (2014), X is the depth below soil surface and A is a factor to account for static or cyclic loading.

$$p_u = \min\{p_{u1}, p_{u2}\} \quad (25)$$

$$p_{u1} = (C_1X + C_2D)\gamma X \quad (26)$$

$$p_{u2} = C_3D\gamma X \quad (27)$$

γ is the submerged unit weight of soil and D is the pile diameter. C_1 , C_2 and C_3 are determined from the graph given in figure F-4 in DNV-OS-J101 (2014).

5.3.2 Material curve in z-direction

The downward resistance is calculated from equation 28 given in DNV-RP-F110 (2007).

$$R_v(z) = \frac{1}{2}N_\gamma\gamma'B(z)^2 + N_q(p'_0 + a)B(z) \quad (28)$$

γ' is the submerged unit weight of soil, p_0 is stress, a is the attraction of soil, $B(z)$ is the contact width of the soil, N_γ is the bearing capacity for soil below the pipe and N_q is the bearing capacity for soil below the pipe. Terzaghi's bearing capacity factors for $\theta = 30$ are used. $N_\gamma = 19.7$ and $N_q = 22.5$.

5.4 Contact elements

Contact elements are used when modelling surfaces that are in contact and transmit forces to each other, but are not attached. The general approach to contact kinematics in SIMLA considers two bodies, A and B. Each body occupies a region in space and has a boundary surface. The bodies displacement fields are denoted $\mathbf{u}^A = \mathbf{u}^A(\mathbf{x}^A)$ and $\mathbf{u}^B = \mathbf{u}^B(\mathbf{x}^B)$ (Sævik, 2008). \mathbf{x} represents the updated coordinates of a point at time t . The initial gap is:

$$g_0 = (\mathbf{x}^B - \mathbf{x}^A)\mathbf{n} \quad (29)$$

where \mathbf{x}^A and \mathbf{x}^B is the the updated coordinates of a point at time t for body B and body A respectively. \mathbf{n} is the outward surface normal vector of body A. After a time increment Δt , the two bodies may be in contact or there will still be a gap opening. g is the current gap at time $t + \Delta t$ in the direction of \mathbf{n} . The definition of gap opening and contact is:

Gap opening:

$$g = (\Delta\mathbf{u}^B - \Delta\mathbf{u}^A)\mathbf{n} + g_0 > 0 \quad (30)$$

Contact:

$$g = (\Delta\mathbf{u}^B - \Delta\mathbf{u}^A)\mathbf{n} + g_0 = 0 \quad (31)$$

5.4.1 Interaction between physical objects and the sea floor

The interaction between physical objects and the sea floor is modelled with CONT126. CONT126 is a one-noded element (Sævik et al., 2016). The element is linked to a predefined contact surface, which in this case is the sea floor. The interaction between the sea floor and the physical objects is modelled with six element groups; one contact element for each of the three segments of the anchor, two for the cable and one for the pipeline. The material properties start to function when a physical object comes into contact with the sea floor. R_CONTACT, which allows a user-defined description of the material curve, is the material type applied to model the contact with the sea floor. The friction coefficients in the x- and y-direction are taken directly from Jónsdóttir (2016). It is recommended in DNVGL-OS-E301 (2015) to use a friction coefficient of 1.0 between the anchor chain and the seabed. The friction coefficient was set to 0.3 between the anchor and the seabed when the anchor was dragged along the y-axis towards the pipeline. The friction coefficient was reduced from 1.0 to 0.3 when the anchor started sliding along the pipeline.

5.4.2 Contact between anchor chain and pipeline

The interaction between the anchor chain and the pipeline is modelled with one roller group. It is assumed that the contact is obtained between a user defined cylinder attached to node one and an arbitrary position between two pipe nodes when three dimensional 3-noded roller elements are used, see figure 10 (Sævik et al., 2016). CONT164 roller elements are used to model the interaction between the cable and the pipeline. The friction coefficient in local XY- direction is 0.50 for the anchor and 0.38 for the anchor chain, as recommended by supervisor Prof. Sævik (Jónsdóttir, 2016). Figure 10 shows the geometrical relations for the roller contact element.

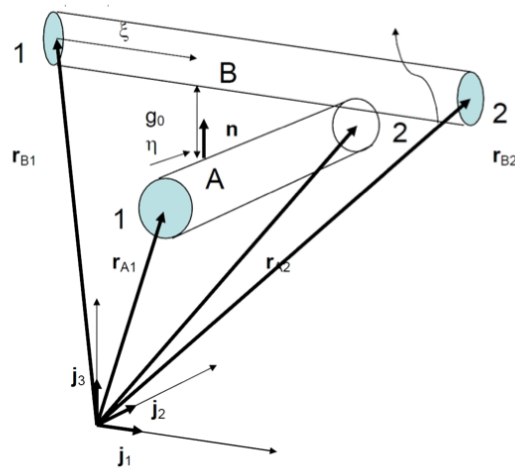


Figure 10: Geometrical relations for roller contact element. Figure: (Sævik, 2008)

The initial gap is expressed by:

$$g_0 = (\mathbf{r}^{B1} - \mathbf{r}^{A1})\mathbf{n} - R^A - R^B \quad (32)$$

where $\mathbf{r}^{\mathbf{A}1}$ represents the updated coordinate position of the roller's first endpoint, $\mathbf{r}^{\mathbf{B}1}$ represents the updated coordinate positions of the pipe's first endpoint, \mathbf{n} is the normal vector, R^A is the roller radii and R^B is the pipe radii (Sævik, 2008).

The current gap at time $t + \Delta t$ in the direction of \mathbf{n} is expressed by:

$$g = (\Delta \mathbf{u}^{\mathbf{B}} - \Delta \mathbf{u}^{\mathbf{A}}) \mathbf{n} + g_0 \quad (33)$$

Contact is established if $g < 0$.

5.4.3 Contact between anchor and pipeline

The contact between the anchor and the pipeline is modelled with the contact element CONT153. CONT153 is a three-noded contact element. The element describes contact between pipe elements and a three-dimensional body (Sævik et al., 2016). The anchor is the three-dimensional body in this case. The contact element is shown in figure 11.

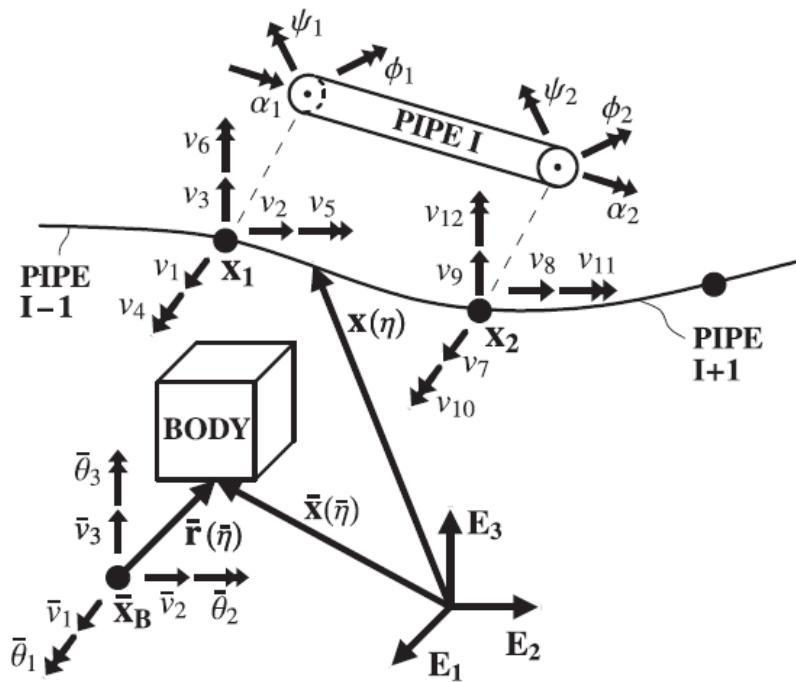


Figure 11: Current configuration of pipe and body (Longva and Sævik, 2013).

CONT153 was developed by Vegard Longva as part of his PhD work. The goal was to develop a robust and efficient contact formulation for the global response prediction of pipelines subjected to interaction with three-dimensional bodies. The contact geometry representation for both the body and the pipeline is continuous providing numerical robustness. The contact kinematics for the pipeline is expressed by means of co-rotated beam theory (Longva and Sævik, 2013). A co-rotated formulation follows the element during deformation. The beam element is considered with reference to a local, element-based coordinate system. The contact kinematics for the rigid body is expressed by means of

straight line parametrization. This formulation leads to a robust contact search in terms of two parameters (Longva and Sævik, 2013).

The contact detection consists of a local and global contact search. If the contact element was inactive in the previous step, i.e. no contact, a global contact search will be performed. The body geometry elements that may obtain contact with the considered pipe element is considered. A local contact search is initiated for the identified elements from the global contact search. The local contact search checks if the conditions for contact are fulfilled (Longva and Sævik, 2013). One contact element can only handle one contact point at the same time. The anchor-pipeline interaction was modelled with three contact elements. This is done to ensure that there are more contact elements than contact points at time t .

The most common contact formulations methods are lagrange multiplier methods, penalty methods and augmented lagrangian method. The lagrange multiplier methods fulfills the non-penetration condition exactly. The penalty method fulfils the non-penetration condition approximately and is more efficient than lagrange methods. The none-penetration condition is also fulfilled when the augmented lagrangian method is used, but only within a prescribed tolerance (Konyukhov and Izi, 2015). The non-penetration condition is defined as:

$$\begin{aligned} \text{Contact:} \quad & p = 0 \quad \text{and} \quad N > 0 \\ \text{No contact:} \quad & p < 0 \quad \text{and} \quad N = 0 \end{aligned} \tag{34}$$

where N is the normal contact force and p is the penetration. The penalty formulation is used for the contact element CONT153. A force with the purpose of eliminating the penetration is introduced at contact points that has penetrated across the target surface for the penalty method (Doyle, 2012).

6 Specifics of analyses

6.1 Comparison study

Simulations were performed to demonstrate the performance of models where CONT153 elements were used. The results of the simulations were compared to Jónsdóttir's (2016) results. The only difference between the models in these analyses was the contact element used to model the contact between the anchor and the pipeline. Jónsdóttir (2016) modelled the anchor pipeline contact with CONT164.

The seabed was not modelled as described in section 5.3 in the comparison study. The material curves used for soil stiffness are taken directly from Wei (2015). Wei (2015) modelled the soil stiffness stiffer than a sea bottom made of normal clay. The anchor and the pipeline will therefore not penetrate the seabed as much as they should and the anchor may have a different attack point on the pipe (Jónsdóttir, 2016). This was the same seabed model as Jónsdóttir (2016) used. The anchor flukes were modelled as circular cylinders. The radius of the circles decreases towards the tip of the fluke creating a pointed tip at the end.

The analysis sequence, which is controlled by the TIMECO card, is static, static, dynamic, dynamic. This is the same sequence as used by Jónsdóttir (2016) in her parametric study. A basic static analysis is performed in the first static sequence. The pipeline is rotated to obtain the desired angle of attack in the second sequence. Figure 12 shows how the angle of attack is defined. The first dynamic analysis runs until the anchor is almost in contact with the pipeline. The time step is reduced in the second dynamic analysis. The time increment between each visual storage was reduced to 0.1 seconds, or 0.01 seconds if necessary. The time increment to be used to reach the required time was 0.01 seconds. The second dynamic analysis allows the anchor to slide along the pipeline if the angle of attack is not 90 degrees. This is achieved by releasing the boundary conditions on the anchor and the anchor chain.

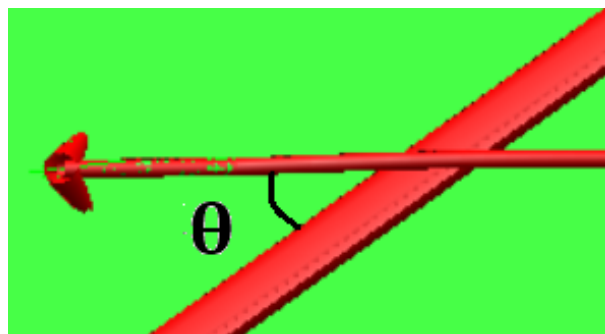


Figure 12: Definition of angle of attack between the pipeline and the anchor.

6.2 Parametric study

The main purpose of the parametric study was to investigate the anchor's behavior in terms of hooking/no-hooking. The pipe was modelled as a ten-meter rigid body as described in section 5.1.1. The time increment used to reach the required time in the dynamic analysis sequence was 0.01 seconds. The parameters investigated are shown in table 18.

The distance from the starting point of the anchor to the pipeline was determined based on the chain length and the vessel velocity.

Table 18: Parameters investigated

Anchor mass [kg]	Anchor class	Anchor chain length [m]	Pipe diameter [inches]	Velocity [knots]	Span height [m]	Slope seabed [deg]
3780	Z	522.5	30	2	0	0
4890	D	550	40	10	2	5
6000	G	577.5				
7800	K	632.5				
9900	O	660				
15400	X	642.5				

The software MATLAB was used to perform the parametric study more efficiently. I received the MATLAB files Jónsdóttir (2016) used in her master thesis. The files were modified, and used to run the parametric study. The main changes were the soil model and how the anchor geometry and contact were modelled. Parameters like damping and sloping seabed were not investigated in Jónsdóttir's (2016) master thesis. These parameters were added to the MATLAB code.

The pipeline was lifted two meters vertically from the seabed to investigate the effect of interaction between an anchor and a pipeline in free span. The effect of partly burying the pipeline below the seafloor was investigated by sinking the pipeline into the seabed. The pipeline was sunk half the pipe diameter into the seabed. The PDISP (prescribed displacement) command was used to prescribe a vertical displacement of the pipeline. The span height was set to 0 when the pipeline was resting on the seabed. This means that the pipeline is resting on top of the seabed, and that the pipeline is not penetrating the seabed as it would do in reality. It is a widely held view that the anchor will hook the pipeline easier if it is towed uphill. The anchor is towed up a hill inclined at 5 degrees with respect to the horizontal to investigate this hypothesis. The effect of friction and damping were investigated for some of the models. This was done to investigate whether damping or increased friction could change the anchor's behavior from not hooking to hooking. The friction coefficient in local XY- direction was changed from 0.50 for the anchor and 0.38 for the anchor chain to 1.0 for both the anchor and the chain. The critical damping is defined as:

$$\omega_0^2 = \frac{k_z}{m} \quad (35)$$

$$c_c = 2m\omega_0 \quad (36)$$

where ω_0 is the natural frequency, k is the stiffness and M is the mass of the anchor. 10 % and 30 % of the critical damping were introduced in the contact elements between the anchor and pipeline to check if damping of the system could change the response from not hooking to hooking.

6.3 Case studies

The main difference between the parametric study and the elastoplastic case studies was the modelling of the pipeline. The pipeline was modelled as ten kilometers long and with PIPE33 elements instead of PIPE31 elements. PIPE33 elements have elastoplastic material properties. The pipeline was only constrained at the end nodes. Only one static analysis was performed in the elastoplastic case study. The coordinates of the rotated pipeline were calculated and implemented directly into the input file. The final dynamic analysis releases the constraints put on the anchor and anchor chain. This allows the anchor to slide along the pipeline.

Cases where the pipeline was resting on the flat seabed, where the pipeline was partly buried and where the pipeline was in free span were investigated in the elastoplastic case studies. The total length of the free span is given in table 19.

Table 19: Span length

Pipe diameter [inches]	Span length [m]
30	50
40	70

Friction between the anchor chain and pipeline was excluded from some of the case studies. The friction induced small motions in the pipeline and the system became unstable. Friction between the anchor chain and the pipeline was therefore removed in some of the case studies (not the parametric study). SIMLA was updated twice during the work with this master thesis. An updated version of SIMLA was downloaded May the 14th, 2017. This version of SIMLA made it possible to include friction between the anchor chain and the pipeline without making the system unstable. Friction between the chain and the pipeline was excluded from the models simulated before this date. Friction between the anchor chain and the pipeline is included in the models where the span height is two meters. The other simulations were not rerun since each simulation was very time consuming.

7 Results and discussion

The same naming system as Jónsdóttir (2016) developed in her master thesis was used in this project. Figure 13 shows how the models are named.

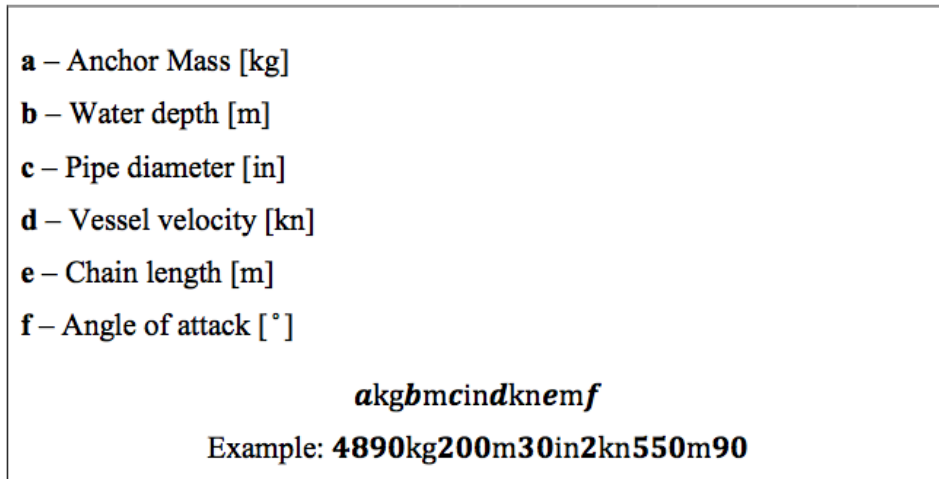


Figure 13: Naming system (Jónsdóttir, 2016)

7.1 Comparison study

There is no clear definition on how to classify the different responses of an anchor-pipeline interaction. Figure 14 shows how the results are categorized in this master thesis.

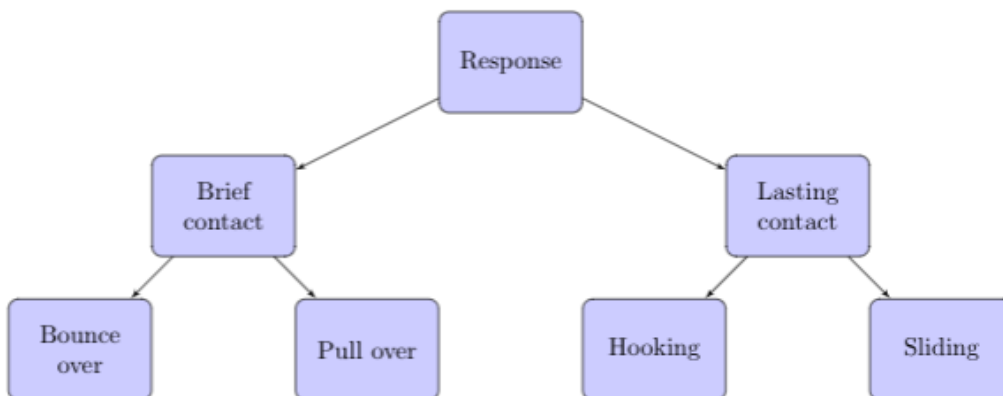


Figure 14: Categorization of the anchor-pipeline interaction.

The anchor-pipeline interaction is defined as either brief contact or lasting contact. Brief contact is defined as either bounce over or pull over. An example of a pull over response is shown in figure 15 and an example of a bounce over response is shown in figure 16. Lasting contact is divided into the categories hooking and sliding. The lasting interaction is defined as hooking if the anchor remains in the same place for several seconds. Jónsdóttir (2016) did also classify the interaction as either realistic or unrealistic. A simulation was said to be unrealistic if the anchor pierced the pipeline, or if the anchor grossly deformed. Jónsdóttir (2016) ignored small deflections at the tip of the anchor flukes and ruled these cases as realistic.



Figure 15: Example of a pull over response

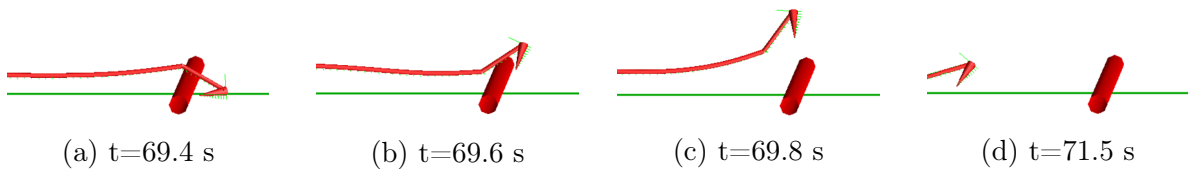


Figure 16: Example of a bounce over response

Eleven SIMLA models, where the anchor geometry and contact were modelled with CONT153, were established. These models have flukes with circular cross section (same geometry as Jónsdóttir (2016) used). The results of the simulations are presented in table 20. The yellow rows are the results from the simulations where the anchor-pipeline contact is modelled with CONT164. These simulations were performed by Jónsdóttir (2016). The purple rows present the results from the simulations where the anchor geometry and contact were modelled with CONT153.

Table 20: Results from simulations, comparison study

	Realistic	Hooking	Sliding	Bounce over	Pull over
6000kg200m	No	No	No	No	Yes
40in2kn578m90	Yes	No	No	No	Yes
6000kg200m	No	Inconclusive			
40in2kn578m60	Yes	No	No	No	Yes
6000kg200m	Yes	-	Yes	No	No
40in2kn578m30	Yes	Yes	Yes	No	No
7800kg200m	No	No	No	No	Yes
40in2kn633m90	Yes	No	No	No	Yes
7800kg200m	No	Inconclusive			
40in2kn633m60	Yes	No	No	No	Yes
7800kg200m	Yes	-	Yes	No	No
40in2kn633m30	Yes	Yes	Yes	No	No
9900kg200m	No	No	No	No	Yes
40in2kn660m90	Yes	No	No	No	Yes
9900kg200m	Inconclusive				
40in2kn660m60	Yes	No	No	No	Yes
9900kg200m	Yes	-	Yes	No	No
40in2kn660m30	Yes	Yes	Yes	No	No
9900kg200m	Yes	No	No	Yes	No
40in10kn660m90	Yes	No	No	Yes	No
15400kg200m	Yes	No	No	Yes	No
40in10kn743m90	Yes	Yes	No	No	No

Both models that showed realistic and unrealistic behavior when the anchor-pipeline contact was modelled with CONT164 were tested. All models showed a realistic behavior when the anchor geometry and contact were modelled with CONT153. Several models showed different behavior when the contact was modelled with CONT153 and with CONT164. One source of error is that the results from the simulations were gathered by visual inspection. Jónsdóttir (2016) did also ignore small deflections at the tip of the anchor flukes and ruled these cases as realistic. The tip of the anchor flukes did not deflect in any of the models where the anchor geometry and contact were modelled with CONT153.

7.2 Parametric study

7.2.1 The pipeline is resting on a flat seabed

The categorization of each model can be found in Appendix A.

Figure 17 shows the hooking ratios for each anchor mass at the water depths 100 and 200 meters.

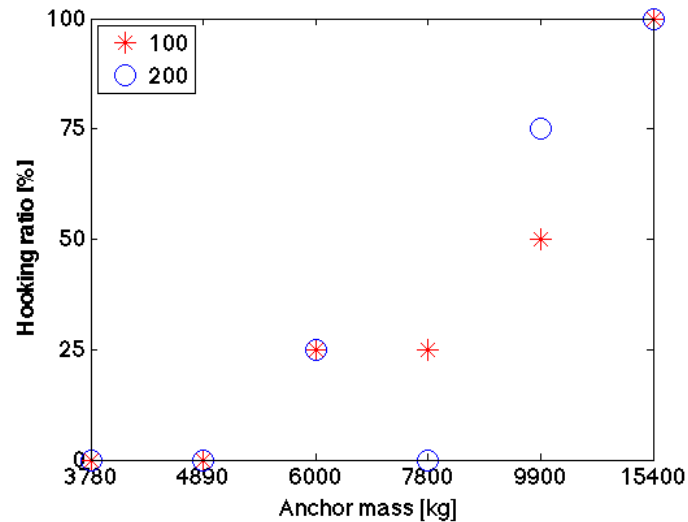


Figure 17: The bar plot shows how the hooking ratio depends on anchor size and water depth when the pipeline is resting on a flat seabed

The trend is that the hooking ratio increases with increasing anchor mass. However, it is not given that a large anchor hooks onto a pipeline even though a smaller anchor did hook onto the same pipeline. Model 6000kg200m30in10kn578m90 (A) hooks the pipeline, while model 7800kg200m30in10kn633m90 (B) is categorized as a bounce over. The differences between these two models are the anchor size and the length of the anchor chain. The own weight of the largest anchor chain, model (B), ensures that the anchor end of the chain lies on the seabed. The weight of the chain keeps the pull angle on the anchor parallel to the seabed. The weight of the anchor shank and anchor chain pull the anchor with a mass of 7800 kg over the pipeline. The length and the own weight of the smallest anchor chain, model (A), are not large enough to ensure that the anchor end of the chain lies on the seabed. This shows that the length and weight of the anchor chain influence whether the anchor hooks onto the pipeline or not. The anchor-pipeline interaction for model (A) and (B) are illustrated in 18 and figure 19 respectively.

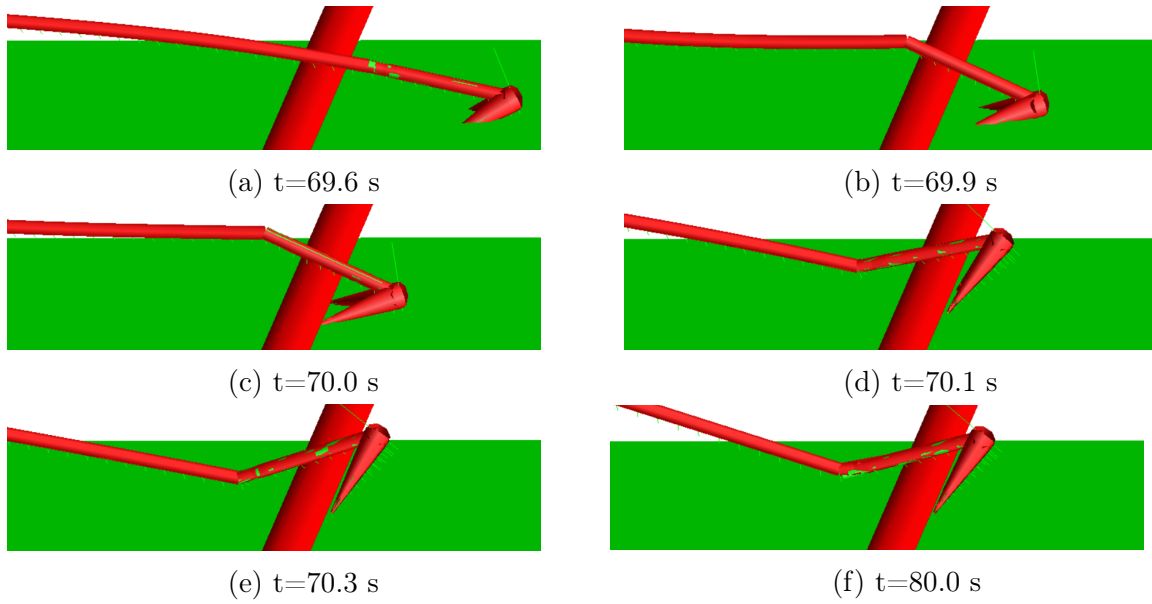


Figure 18: The anchor-pipeline interaction for model 6000kg200m30in10kn578m90 (A)

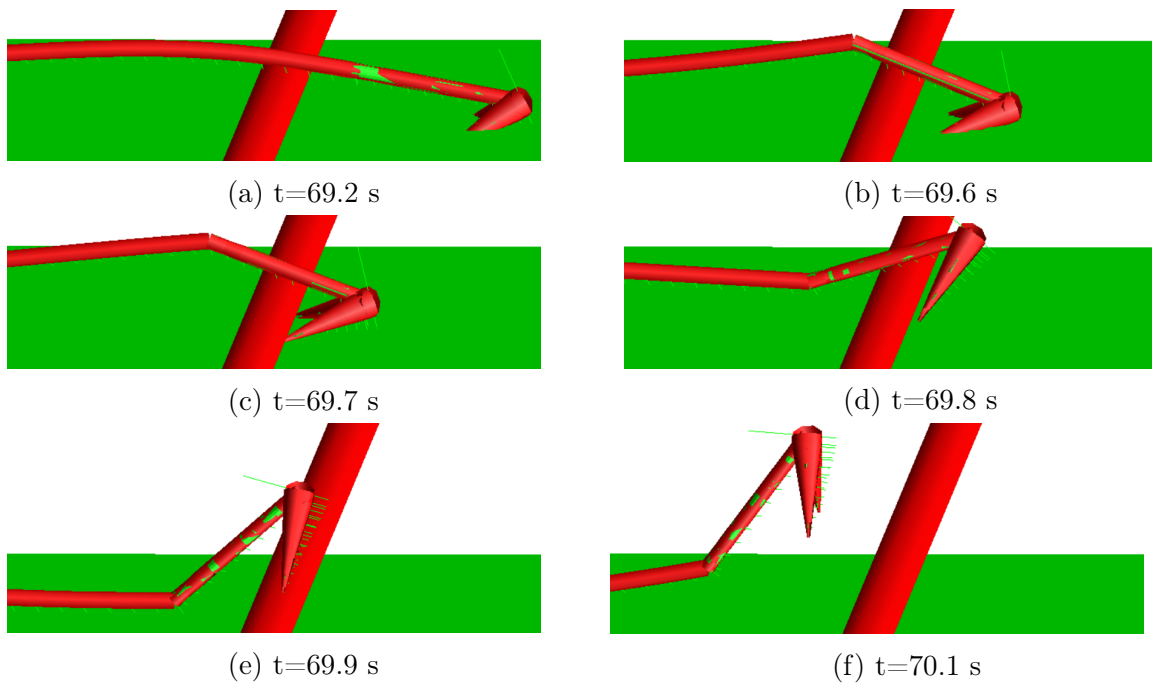


Figure 19: The anchor-pipeline interaction for model 7800kg200m30in10kn633m90 (B)

Figure 20 shows how the hooking ratio depends on the pipe diameter and the vessel velocity. The hooking ratio is significantly higher when the pipe diameter is 30 inches than when the pipe diameter is 40 inches.

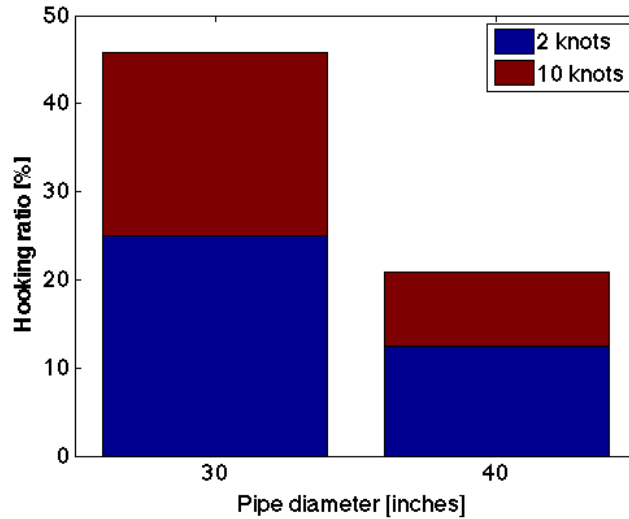


Figure 20: The bar plot shows how the hooking ratio depends on pipe diameter and vessel velocity when the pipeline is resting on a flat seabed.

7.2.2 The span height of the pipeline is two meters and the seabed is flat

The categorization of each model can be found in Appendix B.

Figure 21 shows the hooking ratios for each anchor mass at a water depth of 100 and 200 meters. The hooking ratio for the two smallest anchors is zero. The figure also shows that the hooking ratio does not necessarily increase with increasing anchor mass.

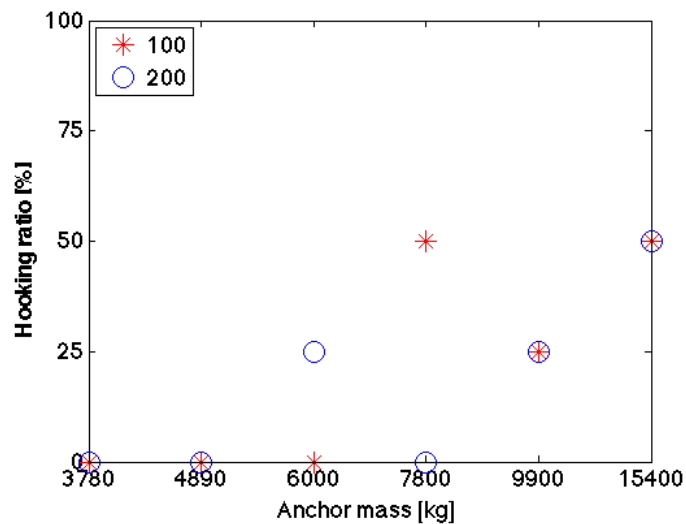


Figure 21: The bar plot shows how the hooking ratio depends on anchor size and water depth when the span height of the pipeline is two meters.

Model 6000kg200m30in2kn578m90 (A) and model 7800kg200m30in2kn633m90 (B) are shown in figure 22 and figure 23 respectively. The differences between these models are the anchor size and the chain length. Model (A), with the smallest anchor size, hooks the pipeline, while model (B) pulls over the pipeline. The own weight of the anchor chain

ensures that the anchor end of the chain lies on the seabed for both models. The weight of the anchor shank pulls the anchor with the larger mass (B) over the pipeline.

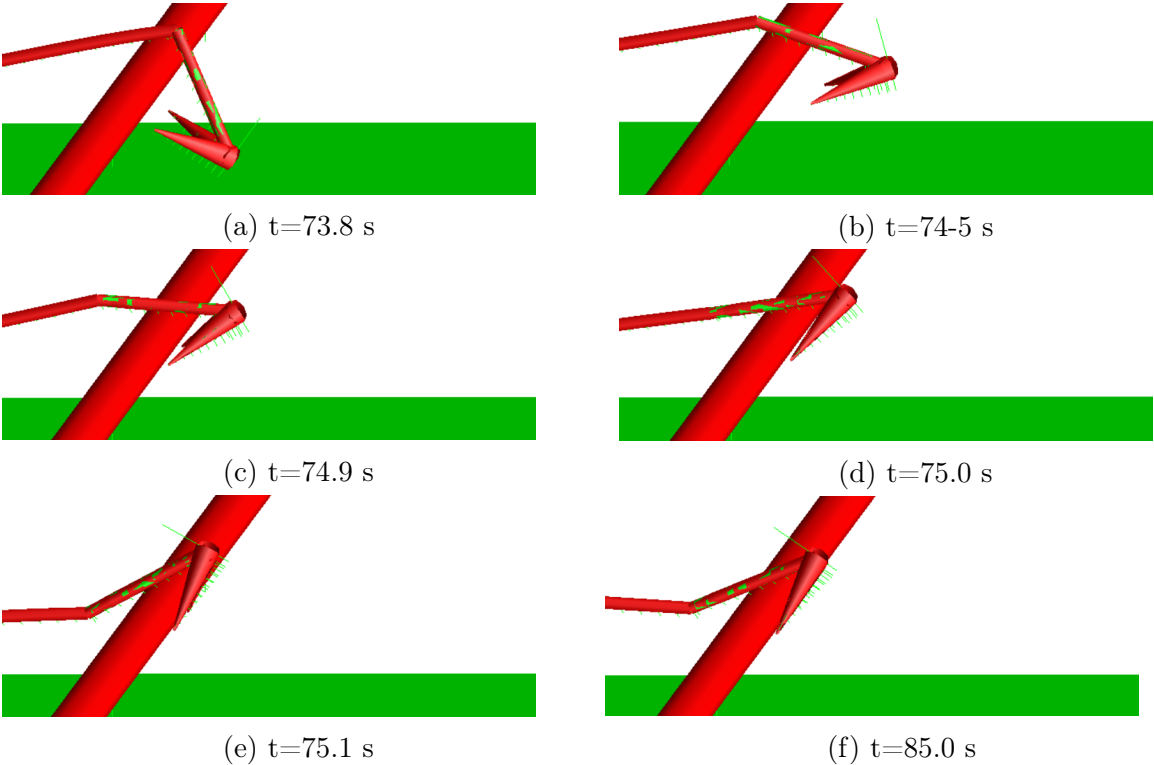


Figure 22: The anchor-pipeline interaction for model 6000kg200m30in2kn578m90

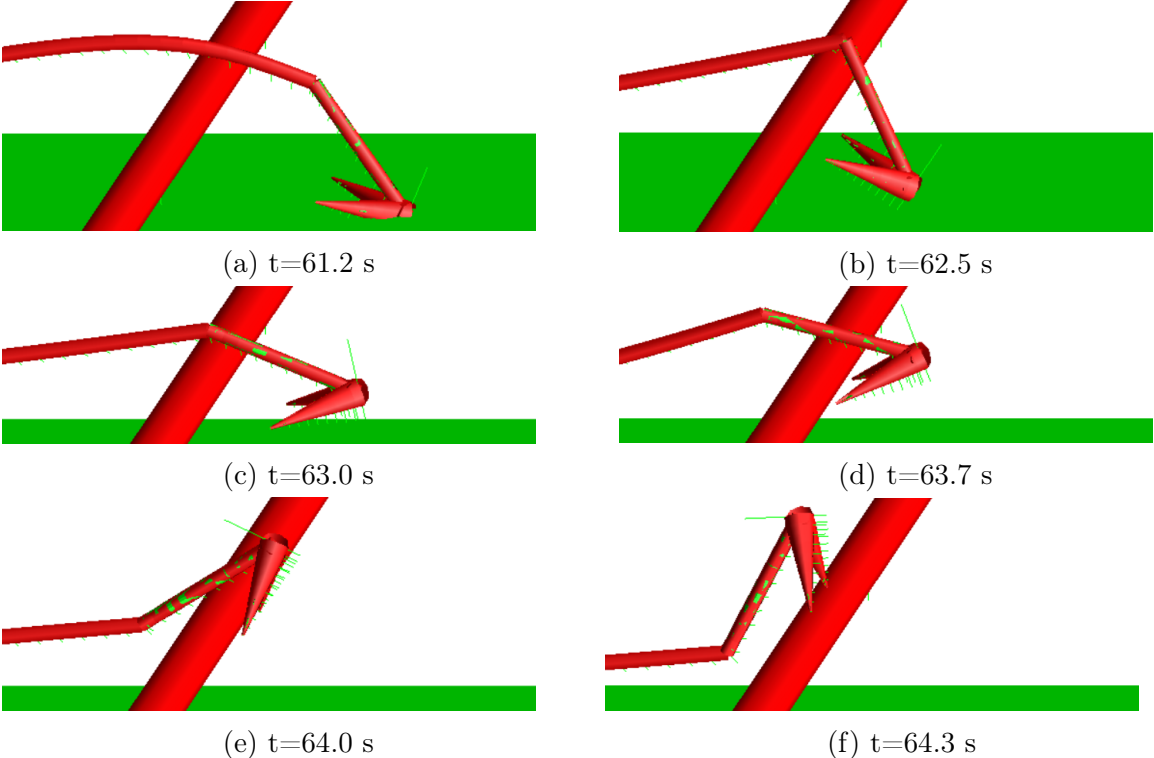


Figure 23: The anchor-pipeline interaction for model 7800kg200m30in2kn633m90

Figure 24 shows how the hooking ratio depends on pipe diameter and the towing speed. The hooking ratio is zero when the vessel velocity is 10 knots.

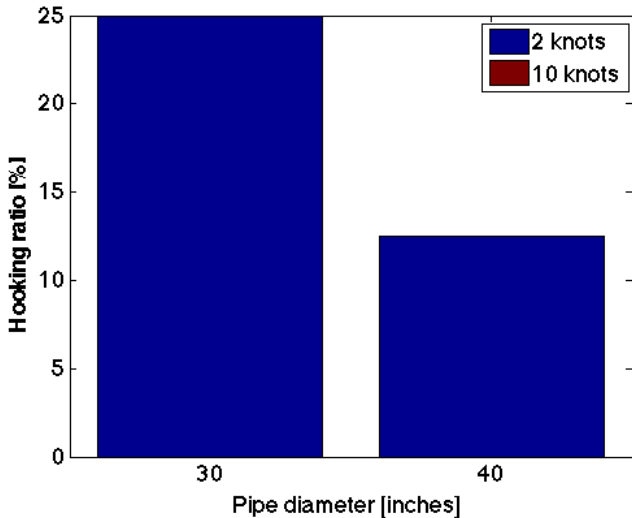


Figure 24: The bar plot shows how the hooking ratio depends on pipe diameter and vessel velocity when the span height of the pipeline is two meters.

All the anchors towed with a velocity of 10 knots bounce over the pipeline. The flukes did never come in a position that made it possible for the pipeline to get stuck between the anchor flukes and the shank. Figure 25 shows how an anchor with a mass of 15400 kg, towed at a speed of 10 knots, bounces over the pipeline. The diameter of the pipeline is 30 inches and the water depth is 200 meters.

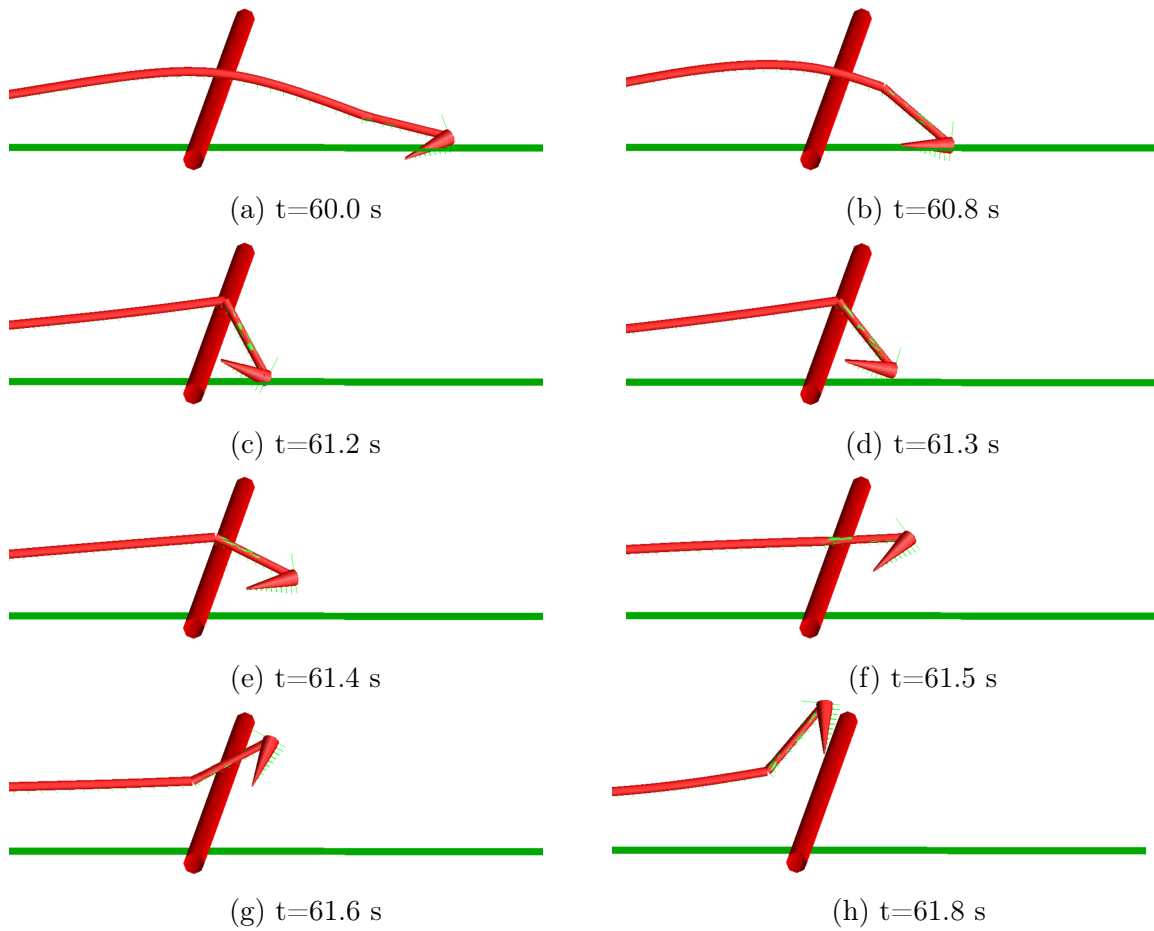


Figure 25: The anchor-pipeline interaction for model 15400kg200m30in10kn743m90

Figure 26 shows the element force in the anchor chain element 50002, which is the chain element closest to the anchor shank.

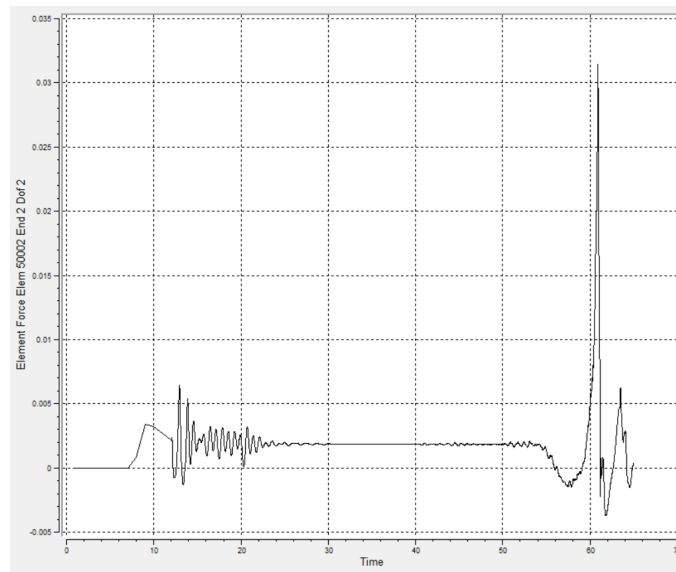


Figure 26: Element force in anchor chain element 50002 for model 15400kg200m30in10kn743m90. The element force is given in megapascal and the time is given in seconds.

The element force in the chain element increases between 60 seconds and 60.6 seconds. Figure 25a shows the position of the anchor when the element force increases. The element force in the anchor chain then decreases rapidly. The position of the flukes shifts from slightly pointing downwards into the soil to slightly pointing upwards. The element force in the anchor chain increase once more as the anchor is lifted off the seabed. The anchor bounces off the pipeline in the time period between 60.5 s and 61.6 s. The force in the anchor chain decreases when the anchor bounces off the pipeline.

7.2.3 The pipeline is partly buried in the seabed

The categorization of each model can be found in Appendix C.

Figure 27 shows the hooking ratios for each anchor mass when the water depth is 100 and 200 meters.

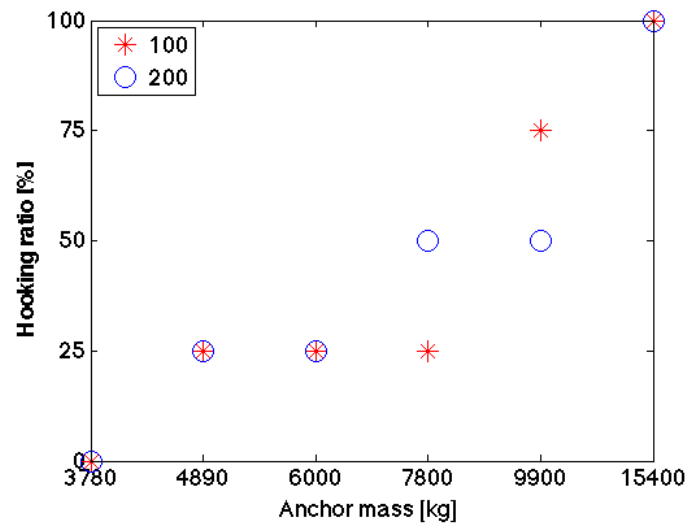


Figure 27: The bar plot shows how the hooking ratio depends on anchor size and water depth when the pipeline is partly buried.

25 % of the anchors with a mass of 4890 kg hook the partly buried pipeline. None of the models, where the anchor mass is 4890 kg, hook the pipeline when the span height is zero or two meters. Figure 28 shows the model 4890kg100m30in2kn550m90 when the pipeline is resting on the sea floor (zero span height) and when the pipeline is partly buried.

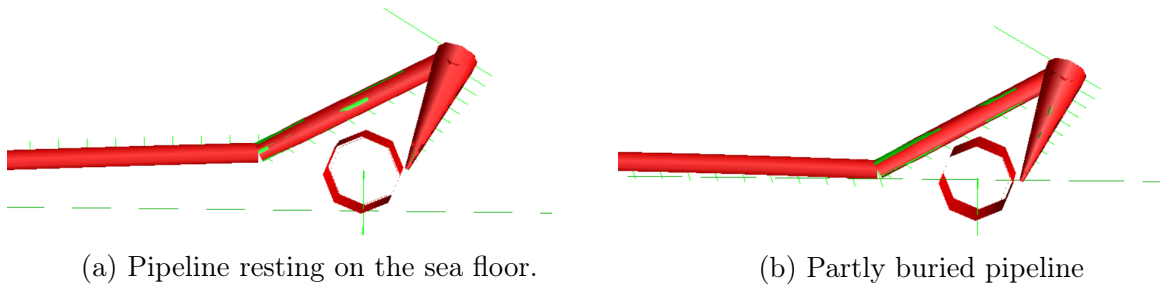


Figure 28: The anchor-pipeline interaction for model 4890kg100m30in2kn550m90

The position of the tip of the flukes relative to the pipe is approximately the same for model (a) and model (b). The anchor chain pulls the anchor shank down towards the sea floor when the pipeline is resting on the seabed. The anchor flukes slide over the pipeline, and the anchor is never in a position that makes it possible to hook the pipeline. Figure 30 shows how the anchor is pulled over the pipeline when the pipeline is resting on the sea floor. The end of the anchor shank is already in contact with the sea floor when the pipeline is partly buried. The anchor flukes cannot be rotated around the pipe when the shank cannot move downwards. The anchor hooks the pipeline. Figure 29 shows how the anchor hooks the pipeline when the pipeline is partly buried in the sea floor.

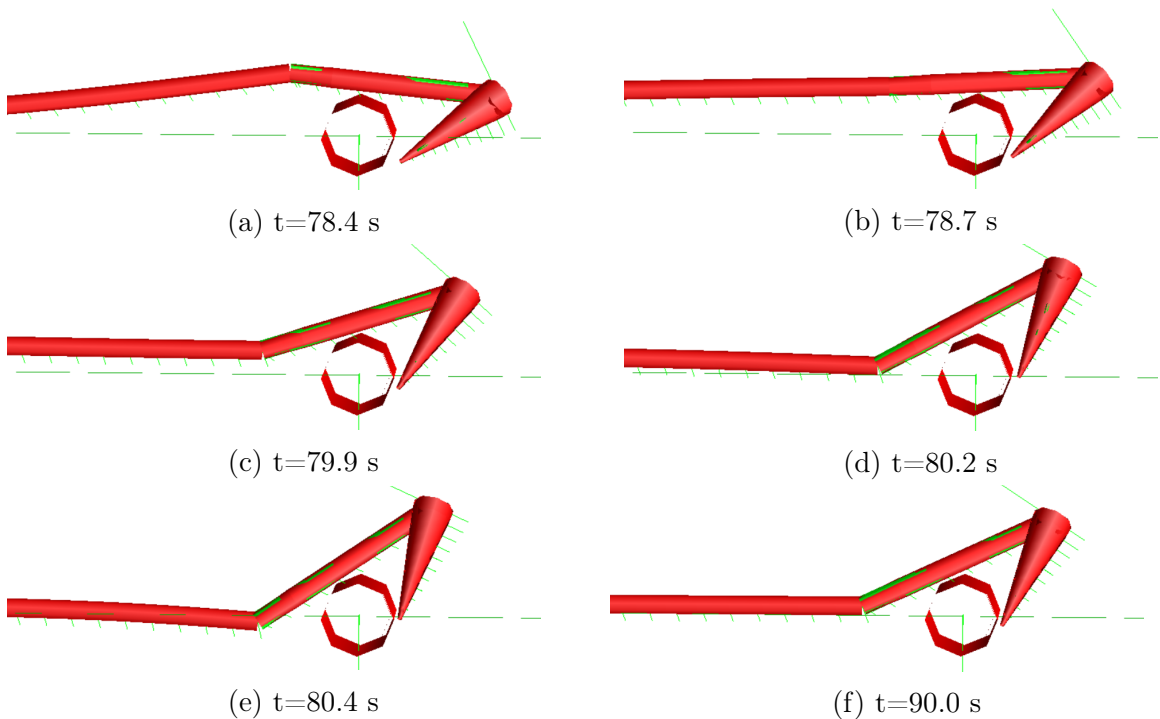


Figure 29: The anchor-pipeline interaction for model 4890kg100m30in2kn550m90. The pipeline is partly buried in the seabed.

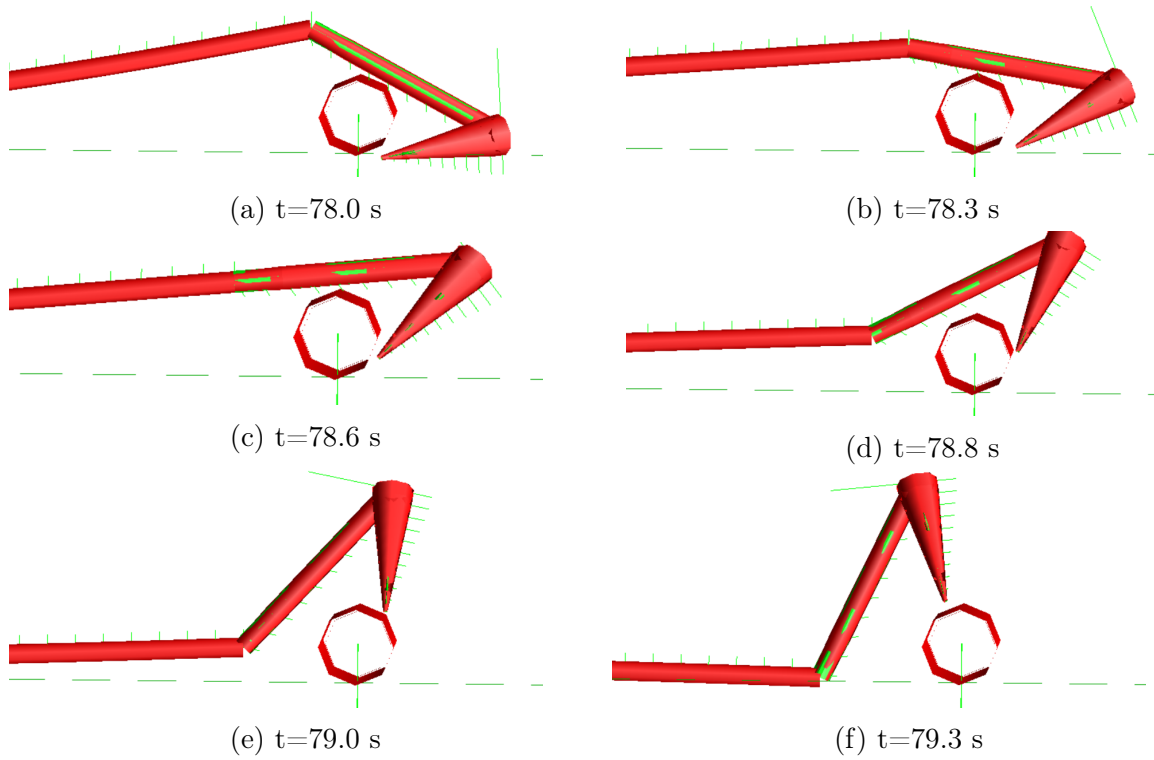


Figure 30: The anchor-pipeline interaction for model 4890kg100m30in2kn550m90. The pipeline is resting on the seabed.

Figure 31 shows how the hooking ratio depend on pipe diameter and towing speed.

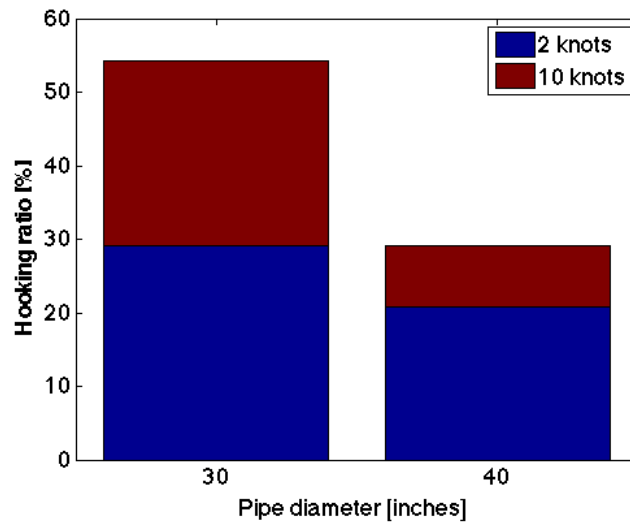


Figure 31: The bar plot shows how the hooking ratio depends on pipe diameter and vessel velocity when the pipeline is partly buried.

7.2.4 The effect of sloping seabed

The categorization of each model can be found in Appendix D.

Figure 32 shows the hooking ratios for each anchor mass at a water depth of 100 and 200 meters. The hooking ratio for the two smallest anchors is zero. The hooking ratio is 100 % when the anchor mass is 15400 kg.

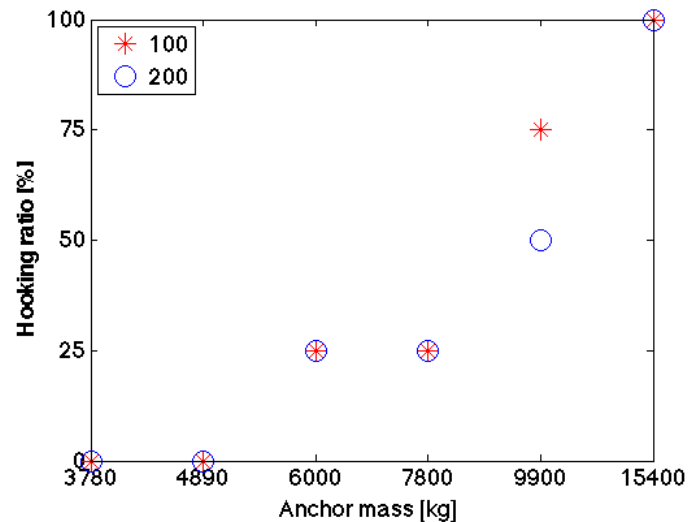


Figure 32: The bar plot shows how the hooking ratio depends on anchor size and water depth when the seabed is inclined at five degrees with respect to the horizontal.

The total hooking ratio when the pipeline was resting on a flat seabed and the angle of attack was 90 degrees was 33.3 %, while the total hooking ratio when the anchor was towed uphill was 35.4 %. The difference in hooking ratio is small. The smallest anchor that hooks onto the pipeline when the anchor is towed uphill is 6000 kg. The reason why smaller anchors are not able to hook onto the pipeline can be explained from figure 28. The anchor shank is not in contact with the seabed when the anchor collides with the pipeline. The weight of the anchor chain pulls the anchor shank towards the seabed and the anchor is rotated over the pipeline.

Figure 33 shows how the hooking ratio depend on pipe diameter and vessel velocity. The hooking ratio increases with decreasing pipe diameter and decreasing vessel velocity.

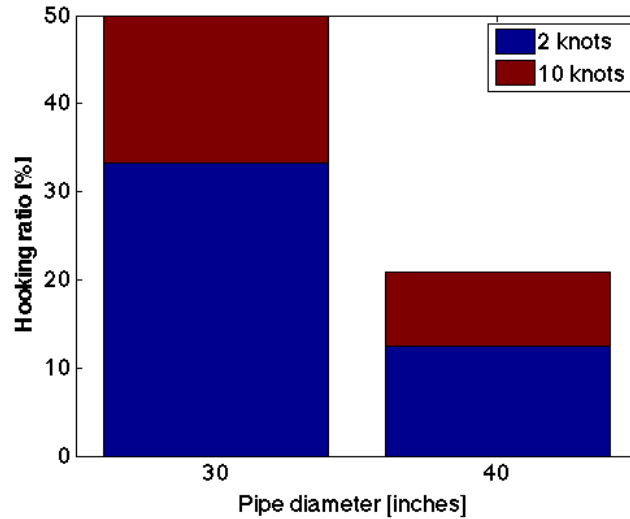


Figure 33: The bar plot shows how the hooking ratio depends on pipe diameter and vessel velocity when the seabed is inclined at five degrees with respect to the horizontal.

7.2.5 30 and 60 degrees angle of attack between the anchor and the pipeline

The categorization of each model can be found in Appendix E. None of the cases hooked onto the pipeline when the angle of attack was 30 or 60 degrees. However, most of the cases experienced sliding along the pipeline. The anchor slides along the pipeline until the anchor chain is tight. The pipeline was originally modelled as ten-meter-long in the parametric study, but the length of the pipeline was extended when necessary to allow the anchor to slide until it was pulled or bounced over the pipeline. Most of the cases, including the anchors towed at a velocity of 10 knots, pulled over the pipeline. This is in contrast to the response when the angle of attack was 90 degrees. Then, the anchor was usually pulled over the pipeline when the anchor was towed at a velocity of 2 knots and bounced over the pipeline when the anchor was towed at a velocity of 10 knots. The anchor did usually twist when the angle of attack was 30 or 60 degrees. The anchor was in the position shown in figure 34 when it was dragged over the pipeline. The flukes were not in contact with the pipeline as the anchor was dragged over it. This caused a smooth crossover, and the response became a pull over.

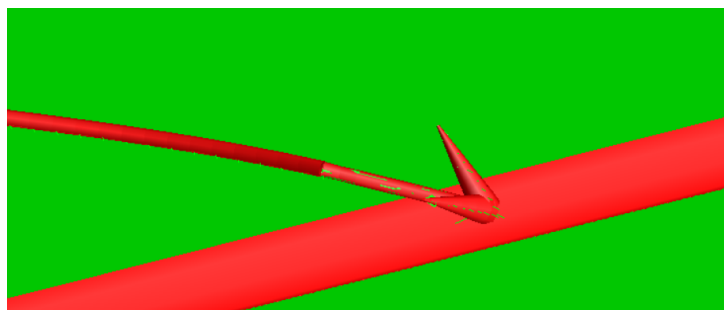


Figure 34: The position of the anchor as it gets dragged over the pipeline. The angle of attack between the anchor and the pipeline is 30 degrees.

Several of the models stopped before it was possible to conclude whether the anchor

would pull over, bounce over or hook the pipeline. The anchor started rotating around its own axis which led to an error in SIMLA. The number of models that was inconclusive increased with decreasing anchor mass. The anchors with the largest anchor masses were pulled over the pipeline and it is therefore likely that the anchors with the smallest masses would also pull over pipeline.

7.2.6 Summary of the parametric study

All the models in the parametric study showed realistic behavior when the contact between the anchor and the pipeline was modelled with CONT153. The anchor flukes did not pierce the pipeline and the tip of the anchor flukes did not deform. The general trend for brief contact was that the anchors pulled over the pipeline when the anchor was towed at a velocity of 2 knots and bounced over the pipeline when the anchor was towed at a velocity of 10 knots. Only cases where the angle of attack between the anchor and the pipeline is 90 degrees are considered in this subsection.

Figure 35 shows the total hooking ratio when the pipeline is resting on the seabed, when the span height is two meters, when the pipeline is partly buried and when the anchor is towed uphill a seabed inclined at five degrees with respect to the horizontal. The hooking ratio is highest when the pipeline is partly buried. Figure 29 shows how small anchors are able to hook the pipeline when the pipeline is partly buried.

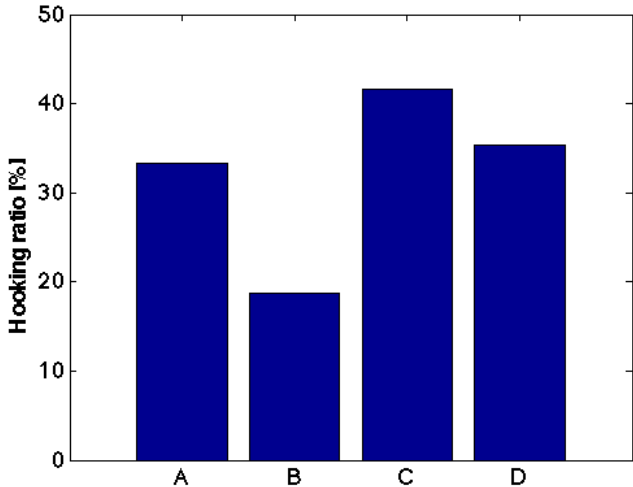


Figure 35: Hooking ratio when the angle of attack is 90 degrees. A: The pipeline is resting on a flat seabed, B: The span height of the pipeline is two meters and the seabed is flat, C: The pipeline is partly buried in a flat seabed, D: The seabed is inclined at five degrees with respect to the horizontal.

Figure 36 shows how the hooking ratio depends on anchor mass. Large anchors are more likely to hook onto a pipeline than small anchors. 84 % of the anchors with a mass of 15400 kg hook the pipeline when the angle of attack is 90 degrees.

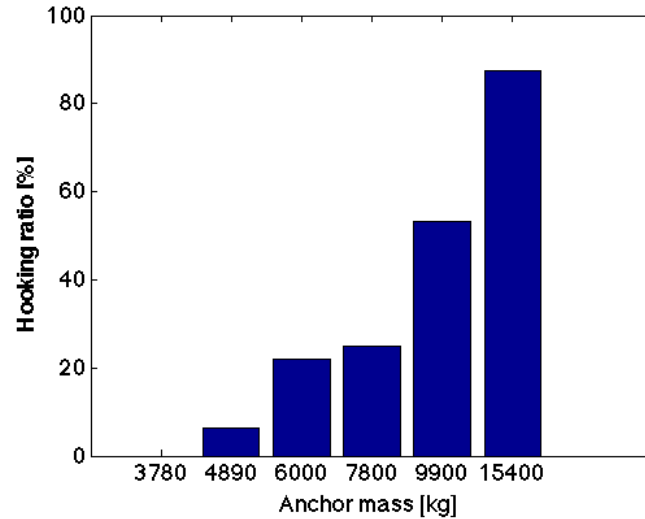


Figure 36: The bar plot shows how the hooking ratio depends on anchor size.

Figure 37 shows the relationship between the hooking ratio and the pipe diameter. An anchor is more likely to hook a 30-inch pipeline than if the pipe diameter is 40 inches. Increasing the pipe diameter decreases the risk of anchor hooking. This trend was also found by Vervik (2011), Wei (2015) and Jónsdóttir (2016). This also consistent with the fact that a larger anchor size increases the risk of anchor hooking.

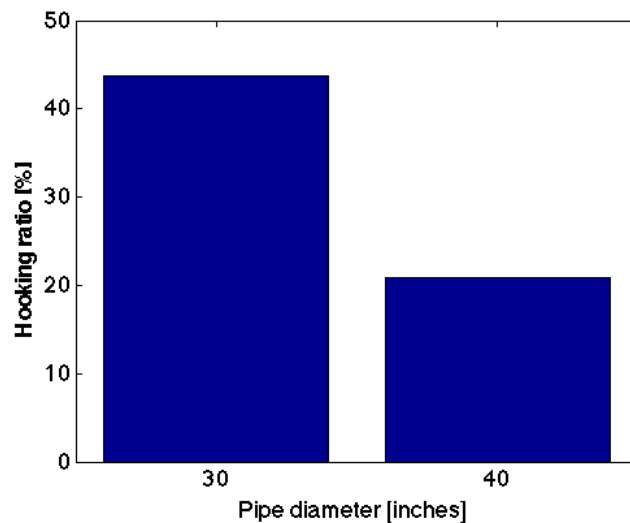


Figure 37: The bar plot shows how the hooking ratio depends on pipe diameter.

The pipe diameter versus the length between the anchor shank and the tip of the anchor fluke is a very important parameter. Vervik (2011) found from geometrical considerations that the smallest anchor that could hook onto a pipeline with a total outer diameter of 0.86 meters falls between the two anchor sizes 3780 kg and 4890 kg. An outer diameter of 0.86 meters corresponds to a coated 30-inch pipeline. The smallest anchor that did hook onto a pipeline with a total outer diameter of 0.86 meters was 4890 kg. However, only 12.5 % of the cases where the anchor was 4890 kg hooked the 30-inch pipeline. None of the cases where the anchor was 3780 kg hooked onto the pipeline, and 50 % of the

anchors with a mass of 6000 kg hooked onto the 30-inch pipeline. An anchor with mass 9900 kg would not be able to hook onto a pipeline with a total outer diameter of 1.12 meter according to the geometrical model described in section 3.2. This model was the same model as Vervik (2011) used in his master thesis. An anchor with a mass of 15400 kg could hook onto a pipeline with a total outer diameter of 1.12 meter according to this model. An outer diameter of 1.12 meters corresponds to a coated 40-inch pipeline. 25 % of the cases where the anchor was 9900 kg hooked onto the 40-inch pipeline and 87.5 % of the cases where the anchor was 15400 kg hooked onto the 40-inch pipeline. This indicates that anchor and pipeline geometry alone cannot predict hooking. Pure geometrical consideration of the anchor hooking event does not consider how the vessel velocity, length of anchor chain, soil stiffness, attack point etc. influence the problem.

Figure 38 shows how vessel velocity affects the hooking ratio. The hooking ratio decreases with increasing vessel velocity. This trend was also found by Wei (2015) and Jónsdóttir (2016).

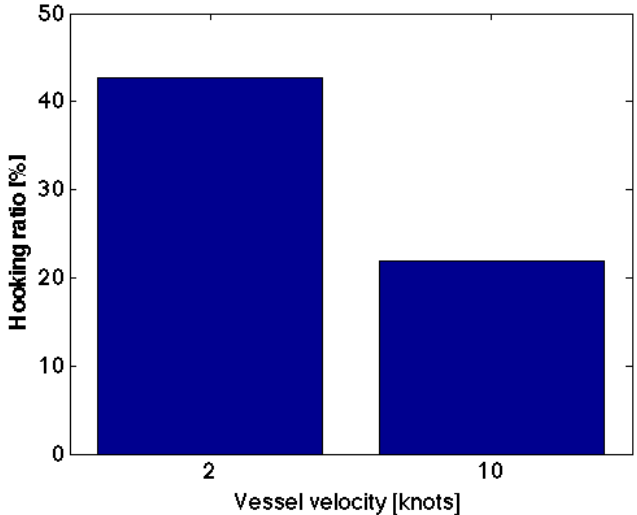


Figure 38: The bar plot shows how the hooking ratio depends on vessel velocity.

Figure 39 shows how the water depth affects the hooking ratio. The main difference between models, where only the water depth differs, is the amount of anchor chain lying on the sea floor. This will in some cases affect the anchor’s attack points on the pipeline.

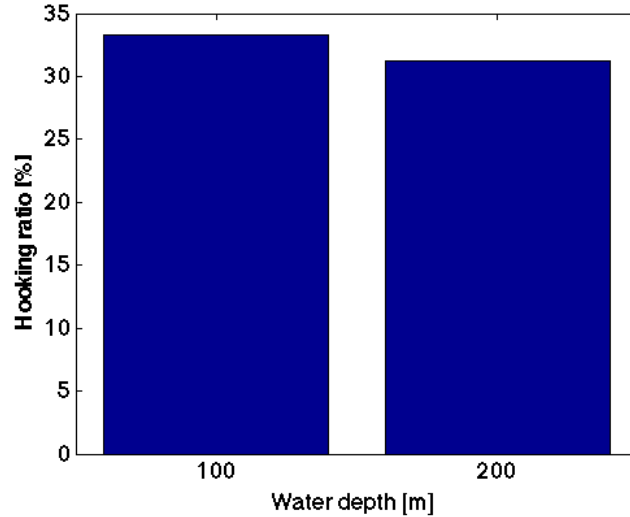


Figure 39: The bar plot shows how the hooking ratio depends on water depth.

The results of the parametric study are quite different from the results obtained in Jónsdóttir (2016) study. She conducted 24 simulations where the angle of attack was 90 degrees. The seabed was flat and pipeline was resting on the seabed. Hooking was reported for only three out of the twenty-four models. Wei (2015) found that approximately one out of two simulations hooked the pipeline when the angle of attack was 90 degrees. However, Wei (2015) investigated different pipe diameters, vessel velocities and span heights. It is therefore not possible to compare the result from the parametric study conducted in this master thesis directly with Wei's (2015) results.

7.2.7 Pipeline forces

The SIMPOST program module is used to post-process the results. Figures 40, 41 and 42 show how the forces inflicted on the pipeline by the anchor and the anchor chain vary with time. The time increment between each visual storage to the .raf file is 0.01 seconds in the time period where the forces vary.

Model 6000kg200m40in10kn578m90 (figure 40) bounces over the pipeline. The duration of the force inflicted by the anchor lasts only 0.5 seconds. The anchor chain comes into contact with the pipeline only a few seconds before the anchor reaches the pipeline. The chain-pipeline contact is the reason why the force in the z-direction is not just one triangular pulse like the force-response in the y-direction. The orientation of the coordinate system can be seen in figure 6.

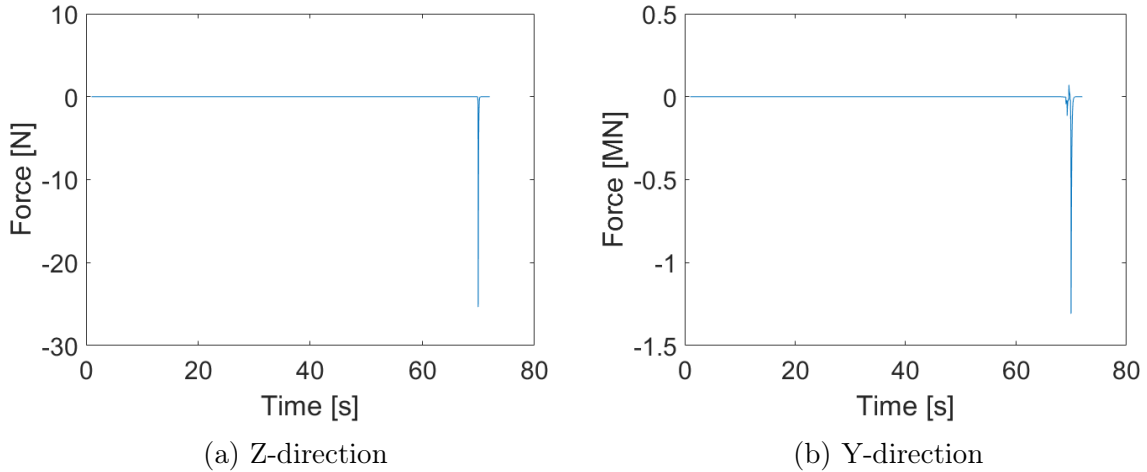


Figure 40: The plot shows how the pipeline forces vary over time for the model 6000kg200m40in10kn578m90.

Model 6000kg100m40in2kn578m90 pulls over the pipeline. The anchor-pipeline contact lasts for 1.8 seconds. The duration of the force response is naturally longer when the anchor pulls over the pipeline than when the anchor bounces over it. Figures 41a and 41b show that the force increases and decreases several times during the time period where the anchor interacts with the pipeline. The reason for this is that the anchor remains in contact with the pipeline while being pulled over it. Figure 41b shows that the anchor chain comes in contact with the pipeline at an earlier time step than for the model that bounces over the pipeline. The water depth is lower and the towing velocity is lower.

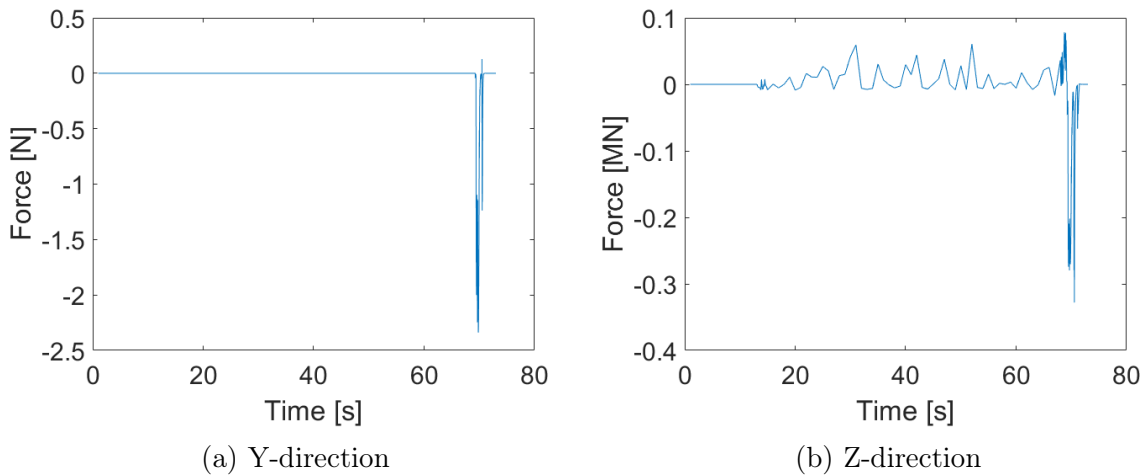


Figure 41: The plot shows how the pipeline forces vary over time for the model 6000kg100m40in2kn578m90.

Model 6000kg100m30in2kn578m90 (figure 42) hooks the pipeline. The forces increase quite slowly because the water depth, the low towing velocity and the own weight of the anchor chain ensure that the anchor end of the chain lies on the seabed for a long time period after the anchor hooks onto the pipeline. The simulation is stopped after 95 seconds

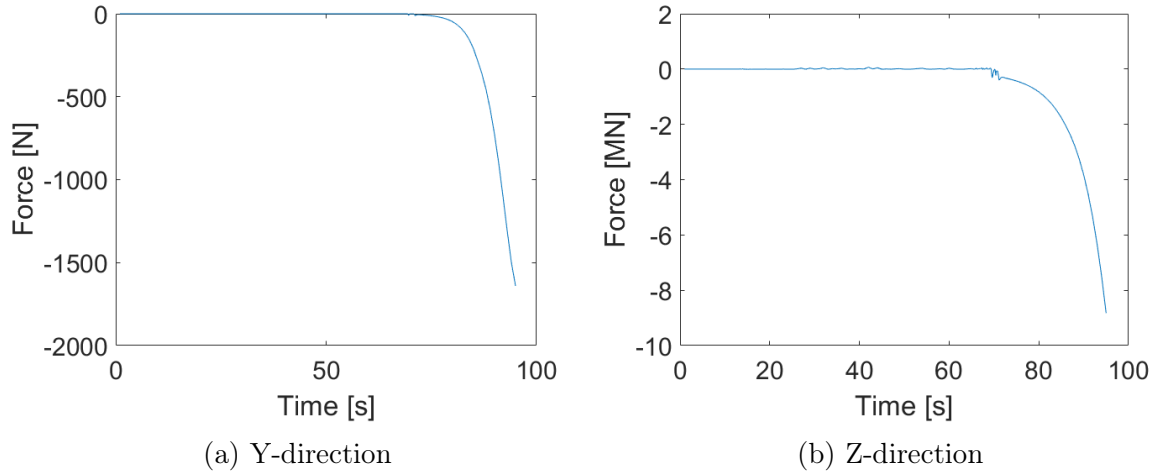


Figure 42: The plot shows how the pipeline forces vary over time for the model 6000kg100m30in2kn578m90.

7.3 Elastoplastic case studies

The purpose of the elastoplastic case studies was to investigate how well the anchor's response had been predicted in the parametric study. The cases inspected were chosen based on the results from the parametric study. Cases where large anchors pulled or bounced over the pipeline in the parametric study were investigated in particular.

15 case studies where the pipeline rested on a flat seabed were performed. Table 21 shows the result of these case studies. The predicted response is the result from the parametric study.

Table 21: Results of the elastoplastic case study. The pipeline is resting on the sea floor.

Case	Response	
	Predicted	Case study
7800kg100m30in2kn633m90	Hooking	Pull over
7800kg100m30in10kn633m90	Bounce over	Hooking
900kg100m40in2kn660m90	Pull over	Pull over
900kg100m40in10kn660m90	Pull over	Bounce over
9900kg200m30in2kn660m30	Pull over	Pull over
9900kg200m30in2kn660m45	-	Pull over
9900kg200m30in2kn660m60	Bounce over	Hooking
9900kg200m30in2kn660m90	Hooking	Hooking
9900kg200m30in10kn660m60	Error	Bounce over
9900kg200m40in2kn660m30	Pull over	Pull over
9900kg200m40in2kn660m60	Pull over	Pull over
9900kg200m40in2kn660m90	Pull over	Pull over
9900kg200m40in10kn660m60	Bounce over	Bounce over
9900kg200m40in10kn660m90	Bounce over	Bounce over
15400kg200m40in10kn743m90	Hooking	Hooking

No hooking response was observed in the parametric study when the angle of attack was 30 or 60 degrees. Elastoplastic case studies were conducted for two cases where the angle of attack was 30 degrees and four cases where the angle of attack was 60 degrees. The model 9000kg200m30in2kn660m hooked onto the pipeline when the angle of attack was 90 and 60 degrees, but not when the angle of attack was 30 degrees. An elastoplastic case study of the same model, but with an angle of attack of 45 degrees, was conducted. The anchor did not hook onto the pipeline when the angle of attack was 45 degrees. The parametric study conducted by Jónsdóttir (2016) indicated that the largest amount of hooking occurred when the angle of attack was 60 degrees. None of the models displayed a hooking response when the angle of attack was 30 degrees. However, the case studies with a global model indicated no hooking response when the angle of attack was 60 degrees. Jónsdóttir (2016) concluded that the rigid modelling of the pipeline, rather than the anchor's response, caused the hooking response in the parametric study.

In general, the parametric study was good at predicting the response of the anchor-pipeline interaction when the pipeline was not in free span. The results of the elastoplastic case studies when the pipeline is partly buried are given in table 22 and the results of the elastoplastic case studies when the span height is two meters are given in table 23.

Table 22: Results of the elastoplastic case studies. The pipeline is partly buried in the seabed.

Case	Response	
	Predicted	Case study
7800kg100m30in10kn633m90	Bounce over	Bounce over
9900kg200m30in2kn660m90	Bounce over	Hooking
9900kg100m40in10kn660m90	Bounce over	Bounce over
9900kg200m40in10kn660m90	Bounce over	Bounce over

Table 23: Results of the elastoplastic case studies. The span height is two meters.

Case	Response	
	Predicted	Case study
7800kg200m30in2kn633m90	Pull over	Bounce over
9900kg200m30in10kn660m90	Bounce over	Bounce over
9900kg200m40in2kn660m90	Pull over	Hooking
15400kg200m30in10kn743m90	Bounce over	Hooking
15400kg200m40in10kn743m90	Bounce over	Hooking

However, some inconsistency between the results obtained from the parametric study and the result from the elastoplastic case study are observed. The parametric study showed that the attack point is an impotent parameter. The pipeline can globally deform in the elastoplastic case studies. The deformation of the pipeline may change the anchor's position relative to the pipeline compared to the parametric study. This is one explanation for the inconsistency between the results obtained in the parametric study and the results from the elastoplastic case studies. One other explanation lies in the modeling of the pipeline. The pipeline was modelled as a ten-meter constrained rigid body in the

parametric study. The rigid modelling of the pipeline, rather than the anchor's response, caused the bounce over response in the parametric study.

Element damping in the contact elements between the pipeline and the anchor was introduced to check if damping could change the response from not hooking to hooking in the parametric study. Four cases that hooked onto the pipeline in the elastoplastic case studies but not in the parametric study were investigated. The results are shown in table 24, 25, 26 and 27.

Table 24: The effect of damping. Model: 7800kg100m30in10kn633m90, The pipeline is resting on a flat seabed.

	Predicted response		Elastoplastic case study
	No damping	10 % of critical damping	
Response	Bounce over	Hooking	Hooking

Table 25: The effect of damping. Model: 9900kg200m30in10kn660m90, the pipeline is partly buried in a flat seabed.

	Predicted response		Elastoplastic case study
	No damping	10 % of critical damping	
Response	Bounce over	Hooking	Hooking

Table 26: The effect of damping. Model: 9900kg200m40in2kn633m90, the span height of the pipeline is two meters and the seabed is flat.

	Predicted response		Elastoplastic case study
	No damping	10 % of critical damping	
Response	Pull over	Hooking	Hooking

Table 27: The effect of damping. Model: 15400kg200m40in10kn743m90, the span height of the pipeline is two meters and the seabed is flat.

	Predicted response			Elastoplastic case study
	No damping	10 % of critical damping	30 % of critical damping	
Response	Bounce over	Bounce over	Bounce over	Hooking

Element damping in the contact elements between the pipeline and the anchor did change the response from not hooking to hooking for some models. However, this observation is based on a very limited number of simulations. It is stated in the problem description that damping of the system in terms of whether the anchors are passing over the free span too easily should be investigated. The results from the elastoplastic case study and the parametric study indicate that the anchor is passing over the free span too easily. No hooking response is observed in the parametric study when the span height is two meters and the towing velocity is 10 knots. The elastoplastic case studies show that an anchor

with mass 15400 kg hooks onto the pipeline when the vessel velocity is ten knots. Element damping was introduced for two models where the span height of the pipeline was two meters. The results indicate that damping could improve the model, but this assumption is based on only two simulations and are therefore uncertain. The friction coefficient in local XY- direction was changed from 0.50 for the anchor and 0.38 for the anchor chain to 1.0 for both the anchor and the chain for the same four cases. Altering the friction coefficients did not change the response of the anchor when it collided with the pipeline.

8 Conclusion

The main goal of this master thesis was to establish SIMLA models for the hooking event using the contact element CONT153 that allows for sliding under friction along the pipeline. 250 short pipe models and 24 long pipe models have been investigated to analyze the anchor-pipeline interaction. The following conclusions are drawn from the analyzes:

- Simulations were performed to demonstrate the performance of the model as compared to Jónsdóttir's (2016) model. Eleven models were established. The anchor-pipeline interaction was realistic for all models where the anchor geometry and contact were modelled with CONT153. Of the eleven models tested, 55 % of the models showed unrealistic behavior when the anchor-pipeline interaction was modelled with CONT164. These results underpins the hypothesis that CONT153 leads to less numerical problems than CONT164 for the anchor-pipeline interaction.
- The probability of an anchor hooking onto a pipeline increases with decreasing vessel speed, decreasing pipe diameter and increasing anchor size. This is in accord with the results found by Jónsdóttir (2016), Wei (2015) and Vervik (2011).
- The trend is that the hooking ratio increases with increasing anchor mass. However, it is not given that a large anchor hooks onto a pipeline even though a smaller anchor did hook onto the same pipeline. The length and weight of the anchor chain influence whether the anchor hooks onto the pipeline or not.
- None of the models hooked the pipeline in the parametric study when the angle of attack between the anchor and the pipeline was 30 or 60 degrees. However, the model 9900kg200m30in2kn660m60 hooked the pipeline when the pipeline was modelled as ten-kilometers-long. The risk of hooking is largest when the angle of attack is 90 degrees. The risk of hooking the pipeline is larger when the angle of attack is 60 degrees than 30 degrees. This conclusion is drawn from a very limited number of analyzes.
- The hooking ratio is highest when the pipeline is partly buried in the seabed. Increasing the span height decreases the hooking ratio. This is in accord with Wei's (2015) results.
- The pipe diameter versus the length between the anchor shank and the tip of the anchor fluke is a very important parameter. However, the results from the parametric study and the case studies show that a pure geometric model is not sufficient to predict whether an anchor will hook onto a pipeline or not.
- The study has shown that the point of attack is an important parameter when deciding whether the anchor hooks onto the pipeline or not. A small change in the point of attack can change the response from pull over or bounce over to hooking or from hooking to pull over or bounce over.
- In general, the parametric study was good at predicting hooking when the pipeline was not in free span. The rigid modelling of the pipeline, rather than the anchor's response, can make the anchor bounce over or pull over the pipeline instead of hooking onto it.

9 Further work

This is the third master thesis, written at the Institute of Marine Technology at NTNU, that focuses on numerical simulation of the anchor hooking event in SIMLA. Jónsdóttir (2016) investigated how an angle of attack between the anchor and the pipeline would affect the anchor hooking ratio. However, it has been shown that modelling the anchor and the contact with CONT153 gives different results than if the anchor-pipeline contact is modelled with CONT164. The effect of angle of attack should be further investigated. Jónsdóttir (2016) did also investigate how the length of the anchor chain influenced the anchor-pipeline interaction. However, simulations were performed for a very limited number of cases. The results from this master thesis show that the anchor chain length is a very important parameter. Two water depths were investigated, but the anchor end of the chain was always in contact with the seabed when the anchor mass was larger than 6000 kg. The influence of anchor chain weight and length should be further investigated. It would also be interesting to compare the results from simulations in SIMLA with real incidents where anchors accidentally collided with pipelines.

Bibliography

- A.I. Al-Warthan, Jin S. Chung, H.P. Huttelmaier, and G.G. W Mustoe. Effect of ship anchor impact in offshore pipeline. *Proceedings of the International Society of Offshore and Polar Engineers Conference*, 1993.
- DNV-OS-F101. Submarine pipeline systems, 2013. URL <http://rules.dnvgl.com/docs/pdf/DNV/codes/docs/2013-10/OS-F101.pdf>.
- DNV-OS-F111. Interference between trawl gear and pipelines, 2014. URL <http://rules.dnvgl.com/docs/pdf/DNV/codes/docs/2014-09/RP-F111.pdf>.
- DNV-OS-J101. Design of offshore wind turbine structures, 2014. URL <https://rules.dnvgl.com/docs/pdf/DNV/codes/docs/2014-05/OS-J101.pdf>.
- DNV-RP-F107. Risk assessment of pipeline protection, 2010. URL <http://rules.dnvgl.com/docs/pdf/DNV/codes/docs/2010-10/RP-F107.pdf>.
- DNV-RP-F110. Global buckling of submarine pipeline, 2007. URL <http://rules.dnvgl.com/docs/pdf/DNV/codes/docs/2007-10/RP-F110.pdf>.
- DNVGL-OS-E301. Position mooring, 2015. URL <http://rules.dnvgl.com/docs/pdf/dnvgl/OS/2015-07/DNVGL-OS-E301.pdf>.
- John Doyle. What are the differences between the contact formulations?, February 2012. URL <http://www.ansys-blog.com/what-are-the-differences-between-the-contact-formulations/>.
- C Hvam, R Bruscht, M Tominez, and L Vitah. Risk of pipe damage from dragging anchors. *Proceedings of the International Society of Offshore and Polar Engineers*, 1990.
- Kristbjörg Edda Jónsdóttir. Simulation of anchor loads on pipelines. *Master thesis, Norwegian University of Science and Technology Department of Marine Technology.*, 2016.
- Piarras Kelly. Hardening, February 2012. URL http://homepages.engineering.auckland.ac.nz/~pkel015/SolidMechanicsBooks/Part_II/08_Plasticity/08_Plasticity_06_Hardening.pdf.
- Alexander Konyukhov and Ridvan Izi. *Introduction to Computational Contact Mechanics: A Geometrical Approach*. Wiley, New Jersey, 2015.
- Ivar Langen and Ragnar Sigbjörnsson. *Dynamisk analyse av konstruksjoner*. Tapir, 1986.
- Vegard Longva and Svein Sævik. A penalty -based contact element for pipe and 3d rigid body interaction. *Engineering Structures*, pages 1580–1592, 2013.
- Torgeir Moan. *Finite element modelling and analysis of marine structures*. Akademika forlag, Marine Technology center. Trondheim, Norway., 2003.
- Nord Stream. Pipeline damage assessment against commercial ship traffic threats in the finnish eez (kalbadagrund corridor re-routing). *G-EN-PIE-REP-102-00072525*, 2008.
- Antonie Oosterkamp, Ljiljana Djapic Oosterkmap, Kouros Mashayekh, and Luigino Vitali. Prediction of responses of a subsea gas pipeline after a full bore rupture. *Proceedings*

- of the International Society of Offshore and Polar Engineers Conference*, pages 313–320, 2013.
- SOTRA. Stockless anchors, 2014a. URL <http://www.sotra.net/products/anchors/stockless-anchors>.
- SOTRA. Stud link chain, 2014b. URL <http://www.sotra.net/products/chains/studlink-common-link>.
- T Sriskandarajah and R Wilkins. Assessment of anchor dragging on gas pipelines. *Proceedings of the International Society of Offshore and Polar Engineers Conference*, 2002.
- Svein Sævik. Simla - theory. *Norwegian Marine Technology Research Institute*, 2008.
- Svein Sævik, Ole David Økland, Gro Sagli Baarholm, and Janne K.Ø. Gjøsteen. Simla version 3.16.0 user manual. *Norwegian Marine Technology Research Institute*, 2016.
- Stian Vervik. Pipeline accidental load analysis. *Master thesis, Norwegian University of Science and Technology Department of Marine Technology.*, 2011.
- Ying Wei. Anchor loads on pipelines. *Master thesis, Norwegian University of Science and Technology Department of Marine Technology.*, 2015.

A Results from parametric study: Pipeline is resting on a flat seabed

Table A.1: Results of th parameric study when the pipeline is resting on a flat seabed

	Hooking	Sliding	Bounce over	Pull over
3780kg100m 30in2kn523m90				X
3780kg100m 30in10kn523m90			X	
3780kg100m 40in2kn523m90				X
3780kg100m 40in10kn523m90			X	
3780kg200m 30in2kn523m90			X	
3780kg200m 30in10kn523m90			X	
3780kg200m 40in2kn523m90				X
3780kg200m 40in10kn523m90			X	
4890kg100m 30in2kn550m90				X
4890kg100m 30in10kn550m90			X	
4890kg100m 40in2kn550m90				X
4890kg100m 40in10kn550m90			X	
4890kg200m 30in2kn550m90			X	
4890kg200m 30in10kn550m90			X	
4890kg200m 40in2kn550m90				X
4890kg200m 40in10kn550m90			X	
6000kg100m 30in2kn578m90	X			
6000kg100m 30in10kn578m90			X	
6000kg100m 40in2kn578m90				X
6000kg100m 40in10kn578m90			X	

6000kg200m 30in2kn578m90		X
6000kg200m 30in10kn578m90	X	
6000kg200m 40in2kn578m90		X
6000kg200m 40in10kn578m90		X
7800kg100m 30in2kn633m90	X	
7800kg100m 30in10kn633m90		X
7800kg100m 40in2kn633m90		X
7800kg100m 40in10kn633m90		X
7800kg200m 30in2kn633m90		X
7800kg200m 30in10kn633m90		X
7800kg200m 40in2kn633m90		X
7800kg200m 40in10kn633m90		X
9900kg100m 30in2kn660m90	X	
9900kg100m 30in10kn660m90	X	
9900kg100m 40in2kn660m90		X
9900kg100m 40in10kn660m90		X
9900kg200m 30in2kn660m90	X	
9900kg200m 30in10kn660m90	X	
9900kg200m 40in2kn660m90	X	
9900kg200m 40in10kn660m90		X
15400kg100m 30in2kn743m90	X	
15400kg100m 30in10kn743m90	X	
15400kg100m 40in2kn743m90	X	

15400kg100m 40in2kn743m90	X
15400kg200m 30in2kn743m90	X
15400kg200m 30in10kn743m90	X
15000kg200m 40in2kn743m90	X
15400kg200m 40in10kn743m90	X

B Results from parametric study: The span height of the pipeline is two meters and the seabed is flat

Table B.1: Results from the parametric study when the span height of the pipeline is two meters and the seabed is flat

	Hooking	Sliding	Bounce over	Pull over
3780kg100m 30in2kn523m90				X
3780kg100m 30in10kn523m90			X	
3780kg100m 40in2kn523m90			X	
3780kg100m 40in10kn523m90			X	
3780kg200m 30in2kn523m90				X
3780kg200m 30in10kn523m90			X	
3780kg200m 40in2kn523m90			X	
3780kg200m 40in10kn523m90			X	
4890kg100m 30in2kn550m90			X	
4890kg200m 30in10kn550m90			X	
4890kg200m 40in2kn550m90				X
4890kg200m 40in10kn550m90			X	
4890kg200m 30in2kn550m90				X
4890kg200m 30in10kn550m90			X	
4890kg200m 40in2kn550m90				X
4890kg200m 40in10kn550m90			X	
6000kg100m 30in2kn578m90				X
6000kg100m 30in10kn578m90			X	
6000kg100m 40in2kn578m90				X

6000kg100m 40in10kn578m90		X
6000kg200m 30in2kn578m90	X	
6000kg200m 30in10kn578m90		X
6000kg200m 40in2kn578m90		X
6000kg200m 40in10kn578m90		X
7800kg100m 30in2kn633m90	X	
7800kg100m 30in10kn633m90		X
7800kg100m 40in2kn633m90	X	
7800kg100m 40in10kn633m90		X
7800kg200m 30in2kn633m90		X
7800kg200m 30in10kn633m90		X
7800kg200m 40in2kn633m90		X
7800kg200m 40in10kn633m90		X
9900kg100m 30in2kn660m90	X	
9900kg100m 30in10kn660m90		X
9900kg100m 40in2kn660m90		X
9900kg100m 40in10kn660m90		X
9900kg200m 30in2kn660m90	X	
9900kg200m 30in10kn660m90		X
9900kg200m 40in2kn660m90		X
9900kg200m 40in10kn660m90		X
15400kg100m 30in2kn743m90	X	
15400kg100m 30in10kn743m90		X

15400kg100m 40in2kn743m90	X	
15400kg100m 40in10kn743m90		X
15400kg200m 30in2kn743m90	X	
15400kg200m 30in10kn743m90		X
15400kg200m 40in2kn743m90	X	
15400kg200m 40in10kn743m90		X

C Results from parametric study: The pipeline is partly buried in the seabed

Table C.1: The results from the parametric study when the seabed is flat and the pipeline is partly buried in the seabed

	Hooking	Sliding	Bounce over	Pull over
3780kg100m 30in2kn523m90			X	
3780kg100m 30in10kn523m90			X	
3780kg100m 40in2kn523m90				X
3780kg100m 40in10kn523m90			X	
3780kg200m 30in2kn523m90			X	
3780kg200m 30in10kn523m90			X	
3780kg200m 40in2kn523m90				X
3780kg200m 40in10kn523m90			X	
4890kg100m 30in2kn550m90	X			
4890kg100m 30in10kn550m90			X	
4890kg100m 40in2kn550m90				X
4890kg100m 40in10kn550m90			X	
4890kg200m 30in2kn550m90				X
4890kg200m 30in10kn550m90	X			
4890kg200m 40in2kn550m90				X
4890kg200m 40in10kn550m90			X	
6000kg100m 30in2kn578m90	X			
6000kg100m 30in10kn578m90			X	
6000kg100m 40in2kn578m90				X

6000kg100m 40in10kn578m90		X
6000kg200m 30in2kn578m90	X	
6000kg200m 30in10kn578m90		X
6000kg200m 40in2kn578m90		X
6000kg200m 40in10kn578m90		X
7800kg100m 30in2kn633m90		X
7800kg100m 30in10kn633m90		X
7800kg100m 40in2kn633m90	X	
7800kg100m 40in10kn633m90		X
7800kg200m 30in2kn633m90	X	
7800kg200m 30in10kn633m90	X	
7800kg200m 40in2kn633m90		X
7800kg200m 40in10kn633m90		X
9900kg100m 30in2kn660m90	X	
9900kg100m 30in10kn660m90	X	
9900kg100m 40in2kn660m90	X	
9900kg100m 40in10kn660m90		X
9900kg200m 30in2kn660m90		X
9900kg200m 30in10kn660m90	X	
9900kg200m 40in2kn660m90	X	
9900kg200m 40in10kn660m90		X
15400kg100m 30in2kn743m90	X	
15400kg100m 30in10kn743m90	X	

15400kg100m 40in2kn743m90	X
15400kg100m 40in10kn743m90	X
15400kg200m 30in2kn743m90	X
15400kg200m 30in10kn743m90	X
15400kg200m 40in2kn743m90	X
15400kg200m 40in10kn743m90	X

D Results from parametric study: Sloping seabed

Table D.1: The results from the parametric study when the seabed is inclined at 5 degrees with respect to the horizontal

	Hooking	Sliding	Bounce over	Pull over
3780kg100m 30in2kn523m90				X
3780kg100m 30in10kn523m90			X	
3780kg100m 40in2kn523m90				X
3780kg100m 40in10kn523m90			X	
3780kg200m 30in2kn523m90				X
3780kg200m 30in10kn523m90			X	
3780kg200m 40in2kn523m90				X
3780kg200m 40in210n523m90			X	
4890kg100m 30in2kn550m90				X
4890kg100m 30in10kn550m90			X	
4890kg100m 40in2kn550m90				X
4890kg100m 40in10kn550m90			X	
4890kg200m 30in2kn550m90				X
4890kg200m 30in10kn550m90			X	
4890kg200m 40in2kn550m90				X
4890kg200m 40in10kn550m90			X	
6000kg100m 30in2kn578m90	X			
6000kg100m 30in10kn578m90			X	
6000kg100m 40in2kn578m90				X
6000kg100m 40in10kn578m90			X	

6000kg200m 30in2kn578m90	X		
6000kg200m 30in10kn578m90		X	
6000kg200m 40in2kn578m90			X
6000kg200m 40in10kn578m90		X	
7800kg100m 30in2kn633m90	X		
7800kg100m 30in10kn633m90		X	
7800kg100m 40in2kn633m90			X
7800kg100m 40in10kn633m90		X	
7800kg200m 30in2kn633m90	X		
7800kg200m 30in10kn633m90		X	
7800kg200m 40in2kn633m90			X
7800kg200m 40in10kn633m90		X	
9900kg100m 30in2kn660m90	X		
9900kg100m 30in10kn660m90	X		
9900kg100m 40in2kn660m90	X		
9900kg100m 40in10kn660m90		X	
9900kg200m 30in2kn660m90	X		
9900kg200m 30in10kn660m90	X		
9900kg200m 40in2kn660m90			X
9900kg200m 40in10kn660m90		X	
15400kg100m 30in2kn743m90	X		
15400kg100m 30in10kn743m90	X		
15400kg100m 40in2kn743m90	X		

15400kg100m 40in10kn743m90	X
15400kg200m 30in2kn743m90	X
15400kg200m 30in10kn743m90	X
15400kg200m 40in2kn743m90	X
15400kg200m 40in2kn743m90	X

E Results from the parametric study: 30 and 60 degrees angle of attack between the anchor and the pipeline

Table E.1: The results of the parametric study when the angle of attack between the anchor and the pipeline is 30 degrees and 60 degrees. The seabed is flat and the pipeline is resting on the sea floor. The cases are labeled "Error" if the simulation stopped before it was possible to conclude whether the anchor would pull over, bounce over or hook the pipeline. The cases are labeled with a * if it is impossible to conclude whether the brief contact was a bounce over or pull over response.

	Hooking	Sliding	Bounce over	Pull over
3780kg200m 30in2kn523m30			Error	
3780kg200m 30in2kn523m60		X		*
3780kg200m 30in10kn523m30			X	
3780kg200m 30in10kn523m60			Error	
3780kg200m 40in2kn523m30			Error	
3780kg200m 40in2kn523m60			Error	
3780kg200m 40in10kn523m30			Error	
3780kg200m 40in10kn523m60			Error	
4890kg200m 30in2kn550m30		X		X
4890kg200m 30in2kn550m60		X		*
4890kg200m 30in10kn550m30			Error	
4890kg200m 30in10kn550m60			Error	
4890kg200m 40in2kn550m30			Error	
4890kg200m 40in2kn550m60		X		X
4890kg200m 40in10kn550m30			Error	
4890kg200m 40in10kn550m60			Error	
6000kg200m		X		

30in2kn578m30		*
6000kg200m		
30in2kn578m60	Error	
6000kg200m		
30in10kn578m30	X	X
6000kg200m		
30in10kn578m60		*
6000kg200m		
40in2kn578m30	X	X
6000kg200m		
40in2kn578m60	X	*
6000kg200m		
40in10kn578m30	Error	
6000kg200m		
40in10kn578m60	Error	
7800kg200m		
30in2kn633m30	Error	
7800kg200m		
30in2kn633m60	X	X
7800kg200m		
30in10kn633m30	Error	
7800kg200m		
30in10kn633m60		X
7800kg200m		
40in2kn633m30	X	X
7800kg200m		
40in2kn633m60	X	X
7800kg200m		
40in10kn633m30	X	X
7800kg200m		
40in10kn633m60	Error	
9900kg200m		
30in2kn660m30	X	X
9900kg200m		
30in2kn660m60	X	*
9900kg200m		
30in10kn660m30	X	X
9900kg200m		
30in10kn660m60	Error	
9900kg200m		
40in2kn660m30	X	X
9900kg200m		
40in2kn660m60	X	X
9900kg200m		
40in10kn660m30	Error	
9900kg200m		
40in10kn660m60		X

15400kg200m 30in2kn743m30	X	*
15400kg200m 30in2kn743m60	X	X
15400kg200m 30in10kn743m30	X	X
15400kg200m 30in10kn743m60	X	X
15400kg200m 40in2kn743m30	Error	
15400kg200m 40in2kn743m60	X	X
15400kg200m 40in10kn743m30	X	X
15400kg200m 40in10kn743m60	X	X

F Calculations for pipe elements

The tables in this appendix are taken directly from Jónsdóttir (2016).

Anchor

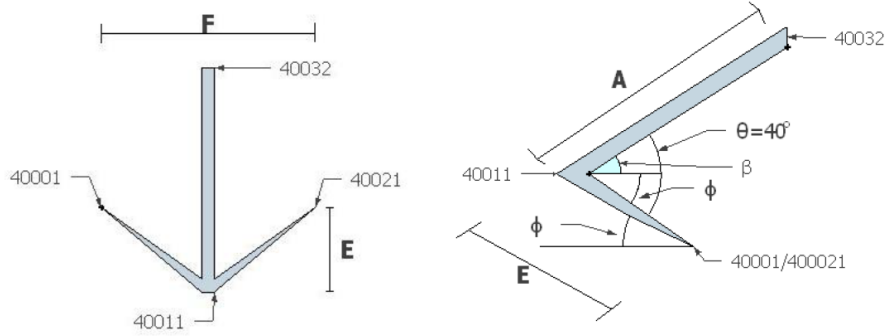


Figure F.1: Simplified Anchor Geometry (Jónsdóttir, 2016)

Table F.1: Anchor calculations

Description	Calculation	
φ	$\varphi = \sin^{-1}\left(\frac{0.2}{E}\right)$	(F-1)
β	$\beta = 40^\circ - \varphi$	(F-2)
Distribution of dry mass	$m_{dry} = \frac{M_{total}}{2\sqrt{\left(\frac{F}{2}\right)^2 + E^2 + A}}$	(F-3)
Distribution of submerged mass	$m_{submerged} = \frac{M_{total} \left(1 - \frac{\rho_{seawater}}{\rho_{steel}}\right)}{2\sqrt{\left(\frac{F}{2}\right)^2 + E^2 + A}}$	(F-4)
Coordinates 40001	$\left[x_0 - \frac{F}{2}, y_0 - E, -depth\right]$	(F-5)
Coordinates 40021	$\left[x_0 + \frac{F}{2}, y_0 - E, -depth\right]$	(F-6)
Coordinates 40011	$\left[x_0, y_0, -depth + 0.2\right]$	(F-7)

Anchor chain

Table F.2: Anchor chain calculations

Description	Calculation	
Radius of chain [m]	$r_c = \frac{ChainDiameter}{2}$	(F-8)
Chain area [m^2]	$A_c = 2\pi r_c^2$	(F-9)
Second moment of inertia [m^4]	$I_c = 2\pi \frac{r_c^4}{4}$	(F-10)
Polar moment of inertia [m^4]	$I_p = 2\pi \frac{r_c^4}{2}$	(F-11)
Axial stiffness [m^4]	$EA = E_{steel}A_c$	(F-12)
Bending stiffness [Nm^2]	$EI = E_{steel}I_c$	(F-13)
Torsion stiffness [Nm^2]	$GI = GI_p$	(F-14)
Chain mass [kg/m]	M_{dry}	(F-15)
Chain volume [m^3/m]	$V_c = \frac{M_{dry}}{\rho_{steel}}$	(F-16)
Buoyancy mass [kg/m]	$M_{buoy} = V_c \rho_{seawater}$	(F-17)
Submerged mass [kg/m]	$M_{sub} = M_{dry} - m_{buoy}$	(F-18)
Damping ratio [-]	$\xi = \frac{c}{c_{critical}}$	(F-19)
Critical damping [$FL^{-1}T^{-1}$]	$c_{critical} = 2\sqrt{mk}$	(F-20)
Damping [$FL^{-1}T^{-1}$]	$c = 2\xi\sqrt{mk}$	(F-21)

Pipeline

Table F.3: Pipeline calculations

Description	Calculation	
Outer diameter steel pipe [m]	c	(F-22)
Thickness of steel wall [m]	$t = \frac{c}{35}$	(F-23)
Outer radius of steel pipe [m]	$r_{sout} = \frac{c}{2}$	(F-24)
Total outer radius of pipe [m]	$R_{out} = r_{sout} + t_{corr} + t_{conc}$	(F-25)
Inner radius [m]	$r_{in} = r_{sout} - t$	(F-26)
Area steel pipe [m ²]	$A_{pipe} = \pi(r_{sout}^2 - r_{in}^2)$	(F-27)
Second moment of inertia [m ⁴]	$I_x = \frac{\pi}{4}(r_{sout}^4 - r_{in}^4)$	(F-28)
Polar moment of inertia [m ⁴]	$I_p = \frac{\pi}{2}(r_{sout}^4 - r_{in}^4)$	(F-29)
Axial stiffness [N]	$EA = E_{steel}A_{pipe}$	(F-30)
Bending stiffness [Nm ²]	$EI = E_{steel}I_x$	(F-31)
Torsion stiffness [Nm ²]	$GI = GI_p$	(F-32)
Steel pipe mass [kg/m]	$m_{steel} = \frac{\pi}{4}(c^2 - (c - 2t)^2)\rho_{steel}$	(F-33)
Corrosion layer mass [kg/m]	$m_{corr} = \pi((r_{sout} + t_{corr})^2 - r_{sout}^2)\rho_{corr}$	(F-34)
Concrete layer mass [kg/m]	$m_{conc} = \pi(R_{out}^2 - 8r_{sout} + t_{corr})^2\rho_{conc}$	(F-35)
Content mass [kg/m]	$m_{cont} = \pi r_n^2 \rho_{cont}$	(F-36)
Buoyancy mass [kg/m]	$m_{buoy} = \pi R_{in}^2 \rho_{seawater}$	(F-37)
Total pipe dry mass [m]	$M_{total} = m_{steel} + m_{corr} + m_{conc} + m_{cont}$	(F-38)
Submerged mass [kg/m]	$m_{sub} = M_{total} - m_{buoy}$	(F-39)

G Electronic appendix

Table G.1: Content of the electronic appendix, uploaded to DIVA

Folder	Content
Parametric study	Contains all the MATLAB files and the input files necessary to run the parametric study. The folder includes a ReadMe.tex for additional information about the MATLAB files and the input files.
Case studies	Contains all the MATLAB files and the input files necessary to run the case studies. The folder includes a ReadMe.tex for additional information about the MATLAB files and the input files.
Poster	Contribution to the Master Thesis Exhibition 2017.